2018 Fall

"Phase Transformation *in* Materials"

11.27.2018

Eun Soo Park

Office: 33-313
Telephone: 880-7221
Email: espark@snu.ac.kr
Office hours: by an appointment

Contents for previous class

< Phase Transformation in Solids >

1) Diffusional Transformation

(a) Precipitation

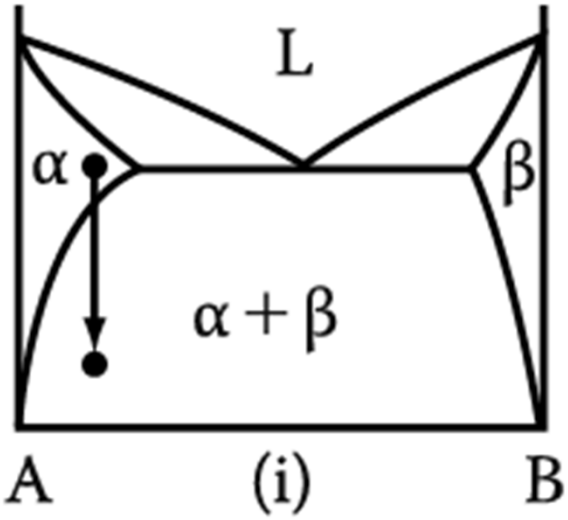

Homogeneous Nucleation

➡ Effect of misfit strain energy

$$\Delta G = -V\Delta G_V + A\gamma + V\Delta G_S$$

$$r^* = \frac{2\gamma}{(\Delta G_V - \Delta G_S)} \qquad \Delta G^* = \frac{16\pi\gamma^3}{3(\Delta G_V - \Delta G_S)^2}$$

$$N_{\text{hom}} = \omega C_0 \exp\left(-\frac{\Delta G_m}{kT}\right)\exp\left(-\frac{\Delta G^*}{kT}\right)$$

Heterogeneous Nucleation

➡ suitable nucleation sites ~ nonequilibrium defects

(creation of nucleus~destruction of a defect($-\Delta G_d$))

$$\Delta G_{het} = -V(\Delta G_V - \Delta G_S) + A\gamma - \Delta G_d$$

$$\frac{\Delta G^*_{het}}{\Delta G^*_{\text{hom}}} = \frac{V^*_{het}}{V^*_{\text{hom}}} = S(\theta)$$

$$\frac{N_{het}}{N_{\text{hom}}} = \frac{C_1}{C_0}\exp\left(\frac{\Delta G^*_{\text{hom}} - \Delta G^*_{het}}{kT}\right)$$

Rate of Homogeneous Nucleation Varies with undercooling below T_e for alloy X_0

Effective equilibrium temperature is reduced by misfit strain E term, ΔGs.

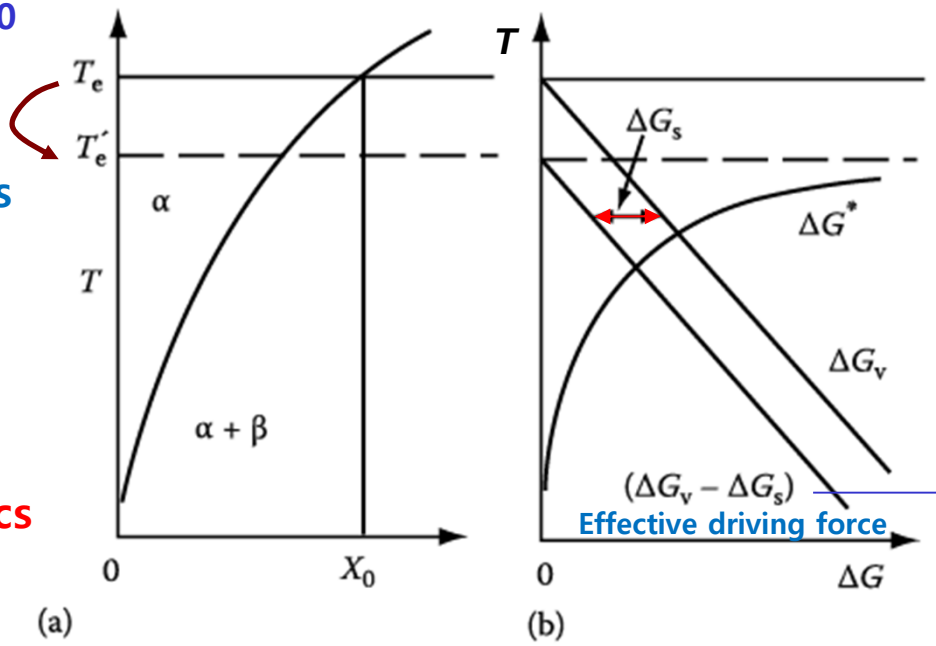

$$\Delta G_V \propto \Delta X \propto \Delta T$$

Composition dependent

$$\Delta G^* = \frac{16\pi\gamma^3}{3(\Delta G_V - \Delta G_S)^2}$$

Resultant energy barrier for nucleation

Thermodynamics

vs

Kinetics

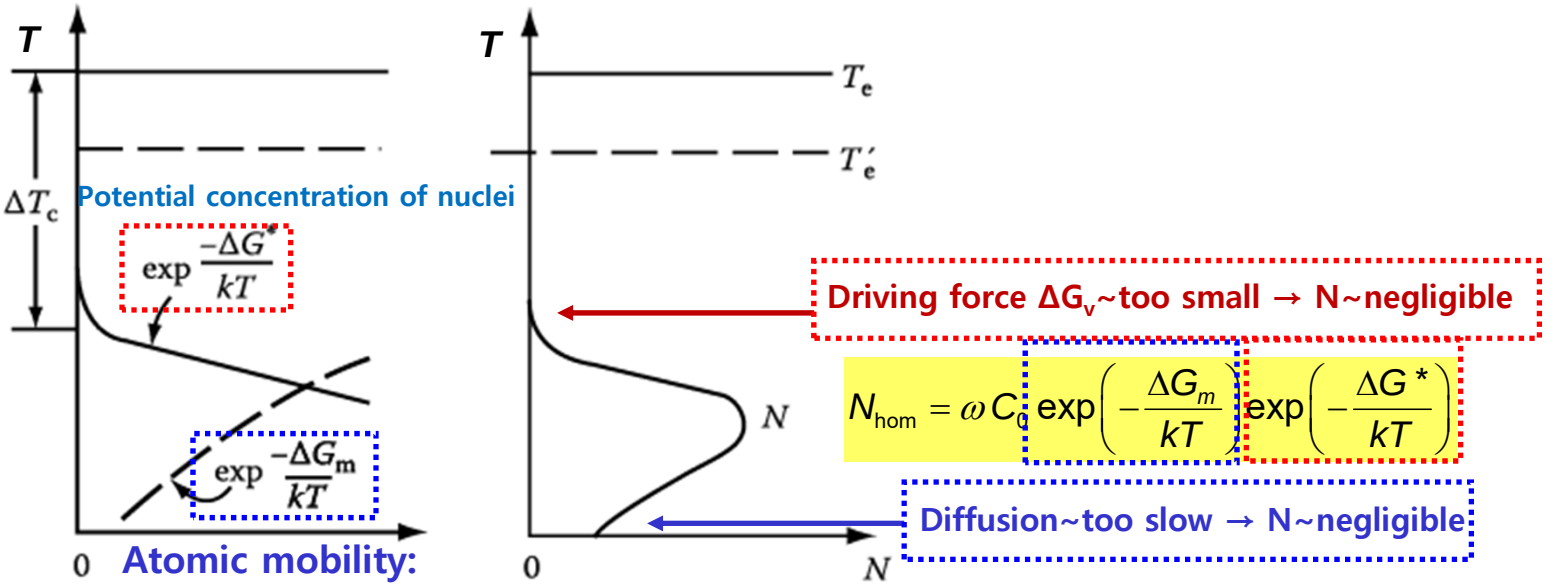

Driving force ΔG_v~too small → N~negligible

$$N_{hom} = \omega C_0 \exp\left(-\frac{\Delta G_m}{kT}\right) \exp\left(-\frac{\Delta G^*}{kT}\right)$$

Diffusion~too slow → N~negligible

Heterogeneous Nucleation in Solids

The Rate of Heterogeneous Nucleation during Precipitation

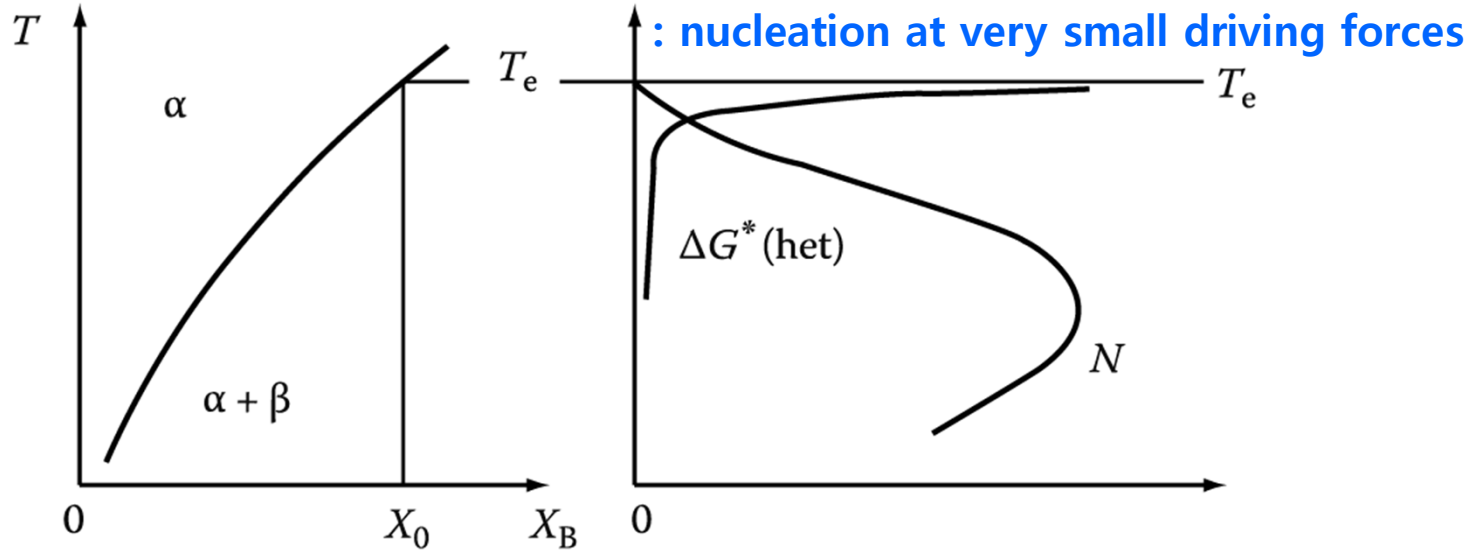

: nucleation at very small driving forces

* Relative magnitudes of the heterogeneous and homogeneous volume nucleation rates

$$\frac{N_{het}}{N_{hom}} = \frac{C_1}{C_0} \exp\left(\frac{\Delta G^*_{hom} - \Delta G^*_{het}}{kT}\right)$$

ω 와 ΔG_m의 차이는 미비하여 무시

ΔG* ~ always smallest for heterogeneous nucleation ⇨ **Exponential factor : very large quantity** ⇨ $\frac{N_{het}}{N_{hom}} > 1$ **High heterogeneous nucleation rate**

But, The factor C_1/C_0 ?

Heterogeneous Nucleation in Solids

$$\frac{N_{het}}{N_{hom}} = \frac{C_1}{C_0}\exp\left(\frac{\Delta G^*_{hom} - \Delta G^*_{het}}{kT}\right)$$

C_1/C_0 for Various Heterogeneous Nucleation Sites

각각의 핵생성처에서 경쟁적으로 핵생성 발생: 구동력 조건에 따라 전체 핵생성 속도에 dominant하게 영향을 미치는 site 변화

Grain boundary	Grain edge	Grain corner	Dislocations		Excess vacancies
$D = 50\ \mu m$	$D = 50\ \mu m$	$D = 50\ \mu m$	$10^5\ mm^{-2}$	$10^8\ mm^{-2}$	$X_v = 10^{-6}$
10^{-5}	10^{-10}	10^{-15}	10^{-8}	10^{-5}	10^{-6}

In order to make nucleation occur exclusively on the grain corner, how should the alloy be cooled?

1) At very small driving forces (ΔG_v), when activation energy barriers for nucleation are high, the highest nucleation rates will be produced by grain-corner nucleation.

핵생성 구동력 ΔG_v ↓ increase

2) dominant nucleation sites: grain edges → grain boundaries

3) At very high driving forces it may be possible for the (C_1/C_0) term to dominate and then homogeneous nucleation provides the highest nucleation rates.

* The above comments concerned nucleation during isothermal transformations
(driving force for nucleation: [isothermal] constant ↔ [continuous cooling] increase with time)

Q4: Precipitate growth:

1) Growth behind Planar Incoherent Interfaces
2) Diffusion Controlled lengthening of Plates or Needles
3) Thickening of Plate-like Precipitates by Ledge Mechanism

5.3 Precipitate Growth

Initial precipitate shape
~minimizes the total interfacial free E

Coherent or semicoherent facets

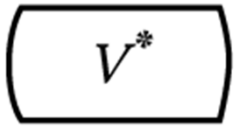

Smoothly curved
incoherent interfaces

Precipitate growth → interface migration
: shape~determined by the relative migration rates

If the nucleus consists of semi-coherent and incoherent interfaces, what would be the growth shape?

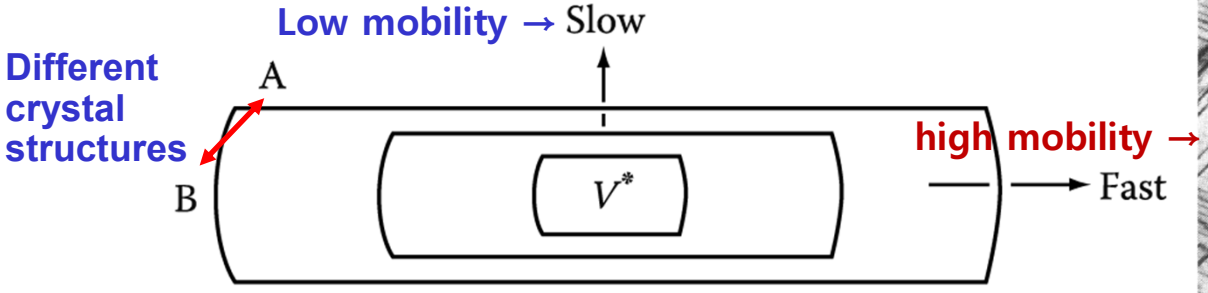

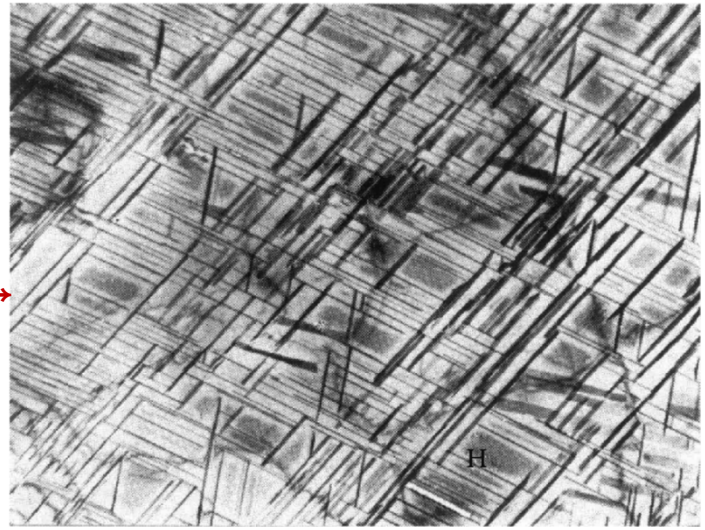

⇨ Ledge mechanism

Thin disk or plate

→ Origin of the Widmanstätten morphology

1) Growth behind Planar Incoherent Interfaces

Incoherent interface → similar to rough interface

→ local equilibrium → diffusion-controlled

Diffusion-Controlled Thickening: precipitate growth rate

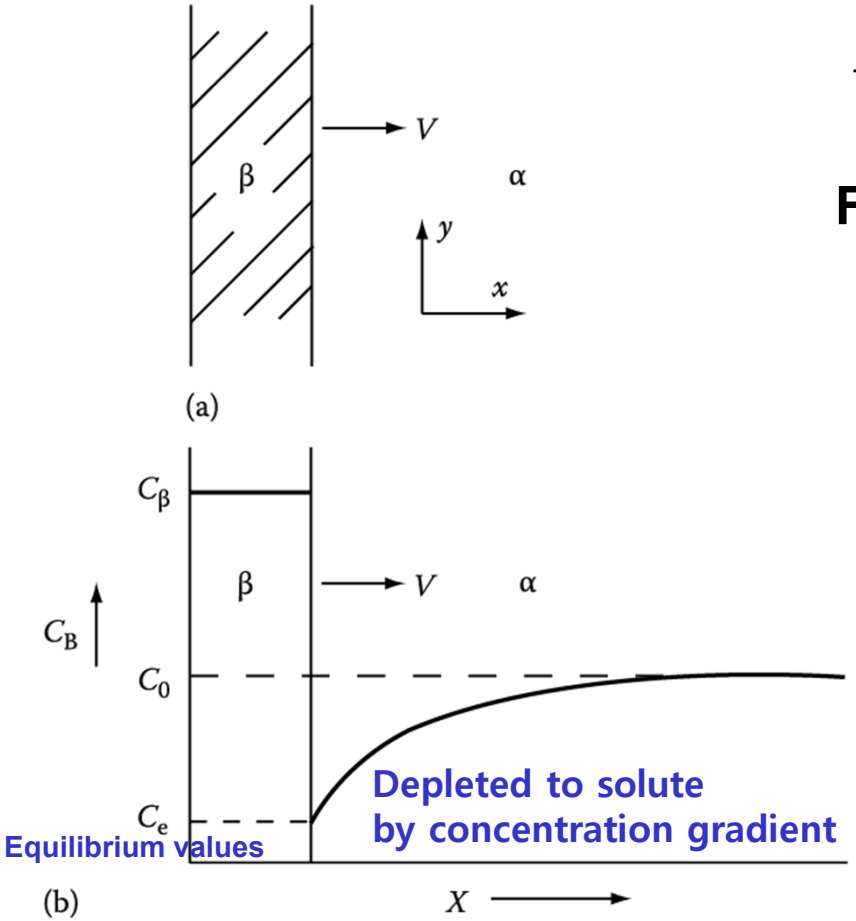

Fig. 5.14 Diffusion-controlled thickening of a precipitate plate.

$$\rightarrow v = f(\Delta T \text{ or } \Delta X, t)$$

From mass conservation,

$$(C_\beta - C_e)dx \text{ mole of } B$$
$$= J_B = D(dC/dx)dt$$

D: interdiffusion coefficient
or interstitial diffusion coeff.

$$v = \frac{dx}{dt} = \frac{D}{C_\beta - C_e} \cdot \frac{dC}{dx}$$

Depends on the concentration gradient at the interface dC/dx

1) Growth behind Planar Incoherent Interfaces

Simplification of concentration profile (Zener)

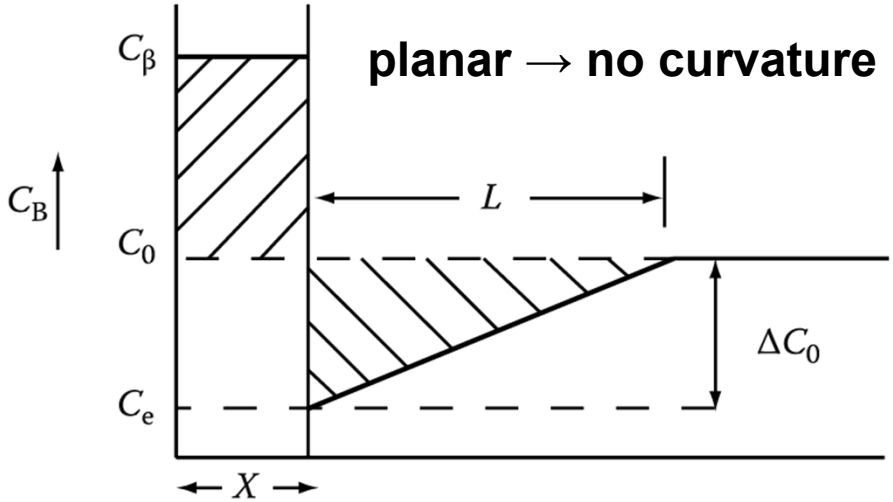

planar → no curvature

Thickness of the slab

$$v = \frac{dx}{dt} = \frac{D}{C_\beta - C_e} \cdot \frac{dC}{dx}$$

$$dC/dx = \Delta C_0 / L \leftarrow L = 2(C_\beta - C_0)x / \Delta C_0$$

$$\because (C_\beta - C_0)x = L\Delta C_0 / 2$$

(same area)

$$v = \frac{D(\Delta C_0)^2}{2(C_\beta - C_e)(C_\beta - C_0)x}$$

if $C_\beta - C_0 \cong C_\beta - C_e$ **and** $X = CV_m$, $\quad \Delta C_0 \rightarrow \Delta X_0 = X_0 - X_e$

(simplification) Mole fractions

$$xdx = \frac{D(\Delta X_0)^2}{2(X_\beta - X_e)^2} dt \xrightarrow{\text{integral}} x = \frac{\Delta X_0}{X_\beta - X_e}\sqrt{(Dt)}$$

Thickness of the slab

$$x \propto \sqrt{(Dt)}$$

Parabolic growth

$$v = \frac{\Delta X_0}{2(X_\beta - X_e)}\sqrt{\frac{D}{t}}$$

$$v \propto \Delta X_0, \quad v \propto \sqrt{(D/t)}$$

Growth rate ∝ supersaturation

1) Growth behind Planar Incoherent Interfaces

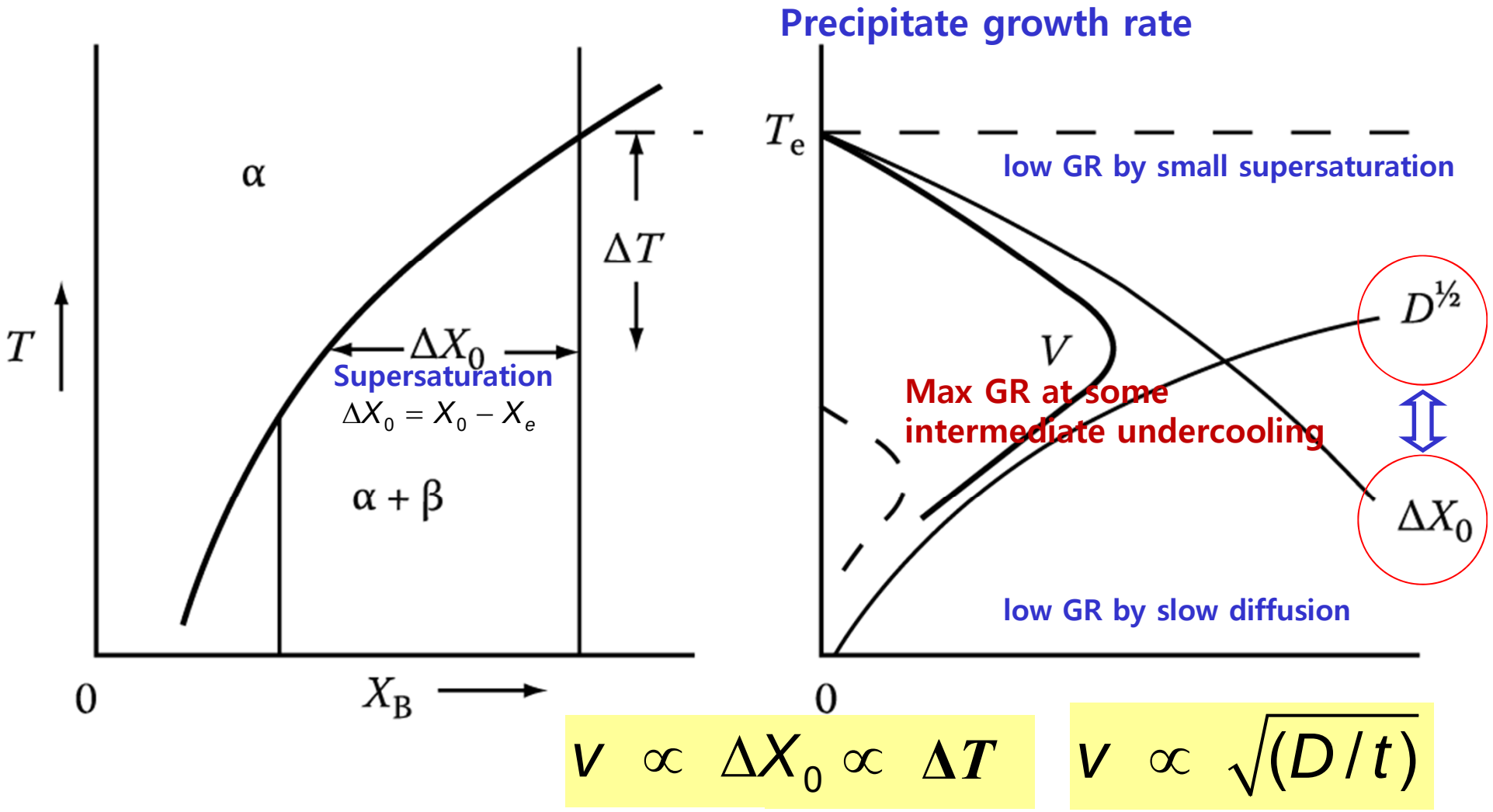

Fig. 5.16 The effect of temperature and position on growth rate, v.

1) Growth behind Planar Incoherent Interfaces

Effect of "Overlap" of Separate Precipitates

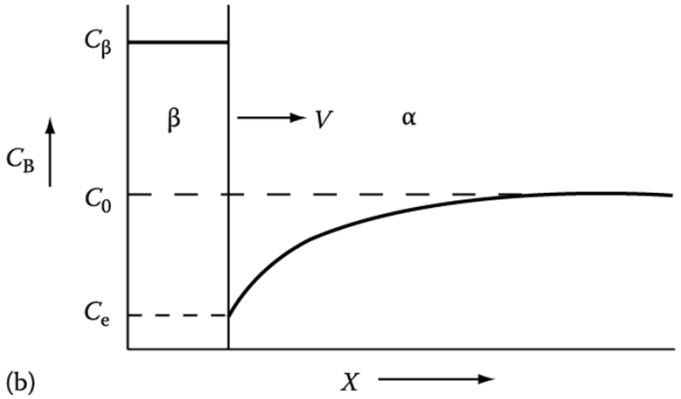

Due to overlapping diffusion fields at later stage of growth, growth will decelerate more rapidly and finally cease when the matrix concentration is X_e everywhere.

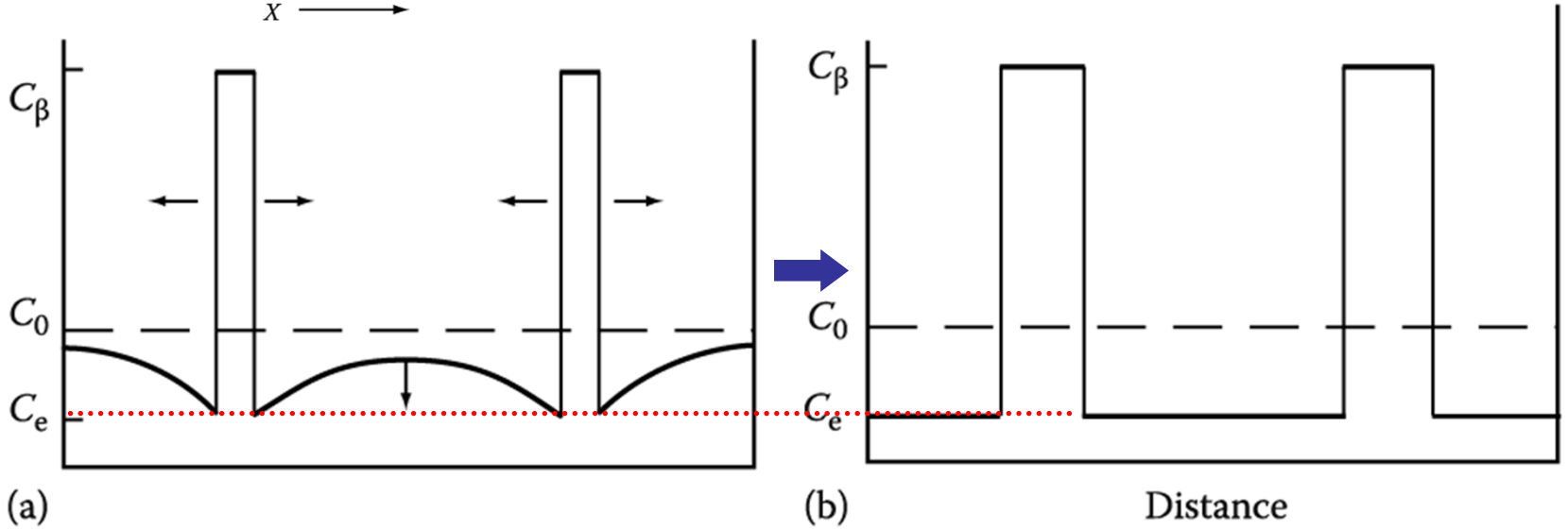

Fig. 5.17 (a) Interference of growing precipitates due to overlapping diffusion fields at later stage of growth. (b) Precipitate has stopped growing.

1) Growth behind Planar Incoherent Interfaces

Grain boundary precipitation ➡ **Faster than allowed by volume diffusion**
involves three steps

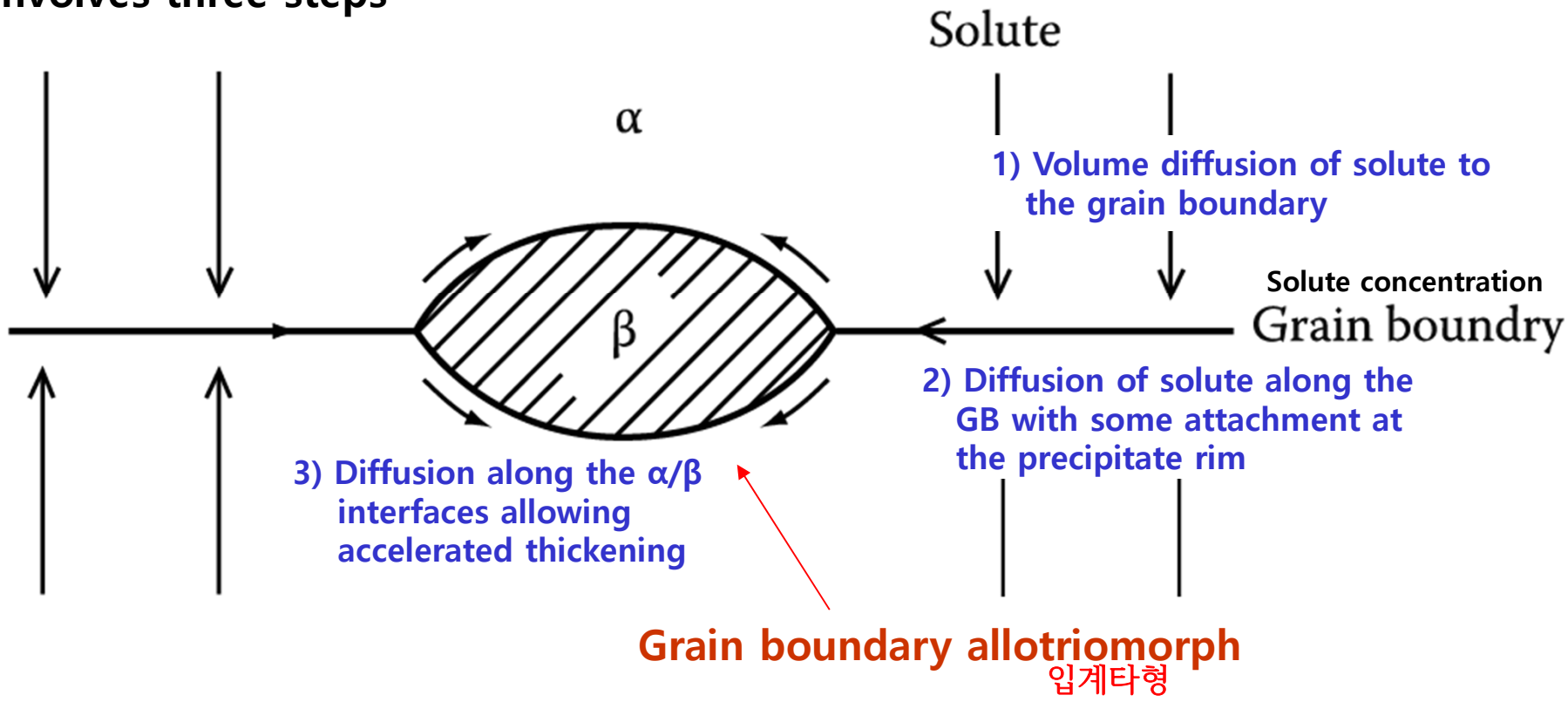

치환형 확산이 일어나는 경우 매우 중요/ 침입형 고용체에서는 체적 확산 속도가 크기 때문에 입계나 전위를 통한 단거리 확산은 상대적으로 중요하지 않음.

Fig. 5.18 Grain-boundary diffusion can lead to rapid lengthening and thickening of grain boundary precipitates, especially by substitutional diffusion.

2) Diffusion Controlled lengthening of Plates or Needles

Plate Precipitate of constant thickness

Volume diffusion-controlled continuous growth process

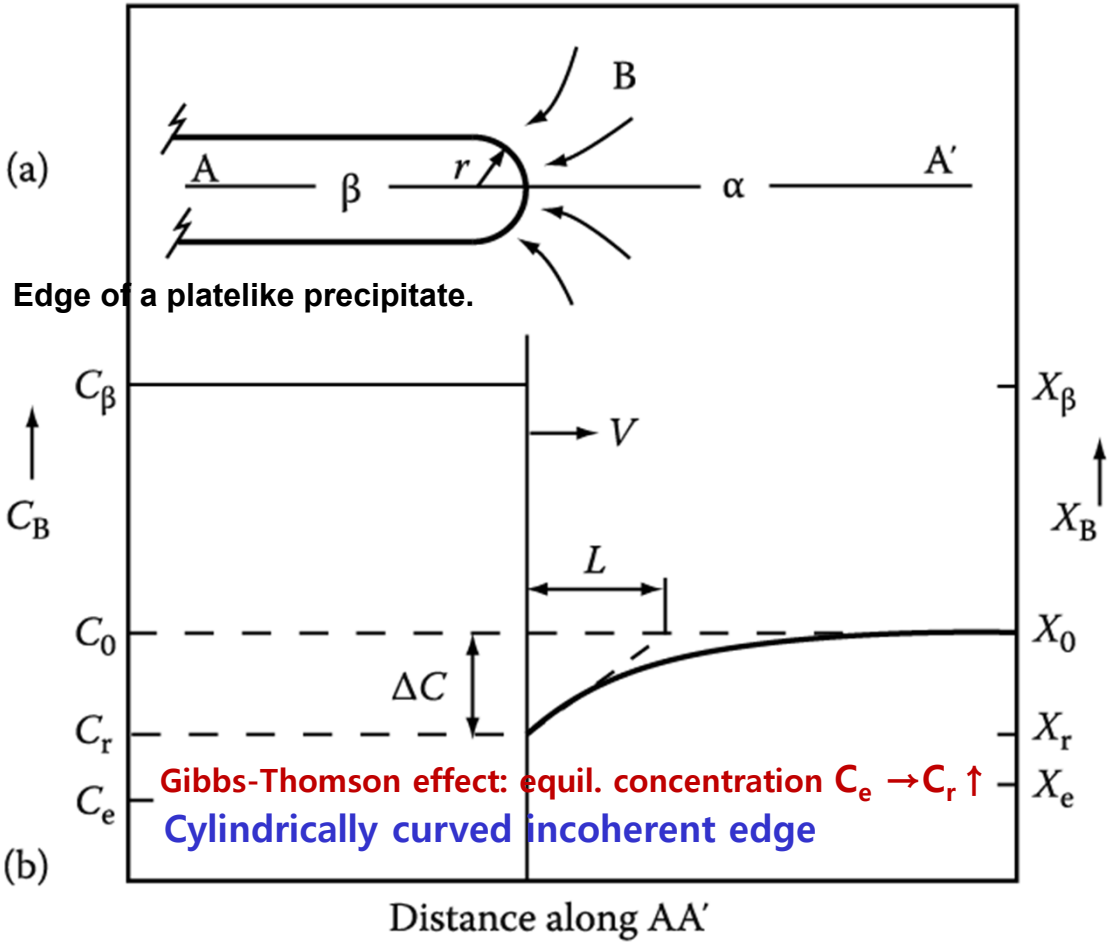

Edge of a platelike precipitate.

Concentration profile along AA' in (a).

From mass conservation,

$$v = \frac{dx}{dt} = \frac{D}{C_\beta - C_e} \cdot \frac{dC}{dx}$$

$$\frac{dC}{dx} = \frac{\Delta C}{L} = \frac{C_0 - C_r}{kr}$$ Radial diffusion

k (const)~1

$$v = \frac{D}{C_\beta - C_r} \cdot \frac{\Delta C}{kr}$$

ΔX for diffusion ∝ edge radius of precipitate (next page)

$$X = CV_m \quad \Delta X = \Delta X_0 \left(1 - \frac{r^*}{r}\right)$$

r*=critical radius (if r=r*, ΔX→0)

$$v = \frac{D\Delta X_0}{k(X_\beta - X_r)} \cdot \frac{1}{r}\left(1 - \frac{r^*}{r}\right)$$

$v \rightarrow$ constant $\rightarrow$ $x \propto t$

(If t=2r, v= constant)

Linear growth

Needle → Gibbs-Thomson increase in G = $2\gamma V_m/r$ instead of $\gamma V_m/r$

→ the same equation but the different value of r^*

2) Diffusion Controlled lengthening of Plates or Needles

Volume diffusion-controlled continuous growth process/ curved ends

The Gibbs-Thomson Effect : curvature of α/β interface~ extra pressure $\Delta P=2\gamma/r$

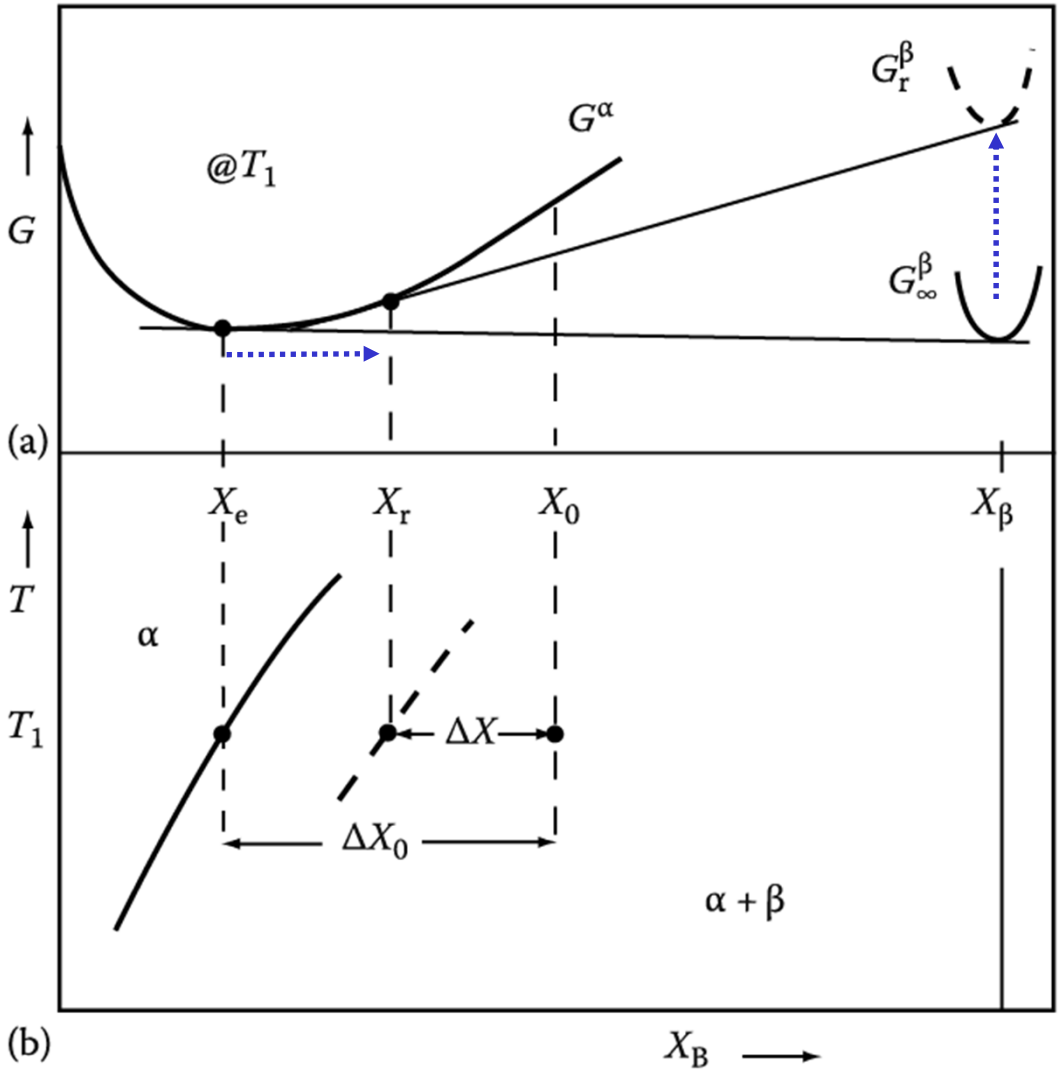

$\Delta G=\Delta P \cdot V \sim 2\gamma V_m/r$ ↑

Interfacial E → total free E ↑

$$\Delta X = \Delta X_0\left(1-\frac{r^*}{r}\right)$$

r^*: critical nucleus, radius

$$\Delta X = X_0 - X_r$$
$$\Delta X_0 = X_0 - X_e$$

r ↑ ⟶ ΔX ↑

* In platelike precipitates, the edges are often faceted and observed to migrate by a ledge mechanism.

Fig. 5.20 Gibbs-Thomson effect.(a) Free E curves at T1. (b) corresponding phase diagram.

2) Diffusion Controlled lengthening of Plates or Needles

Plate Precipitate of constant thickness

Volume diffusion-controlled continuous growth process

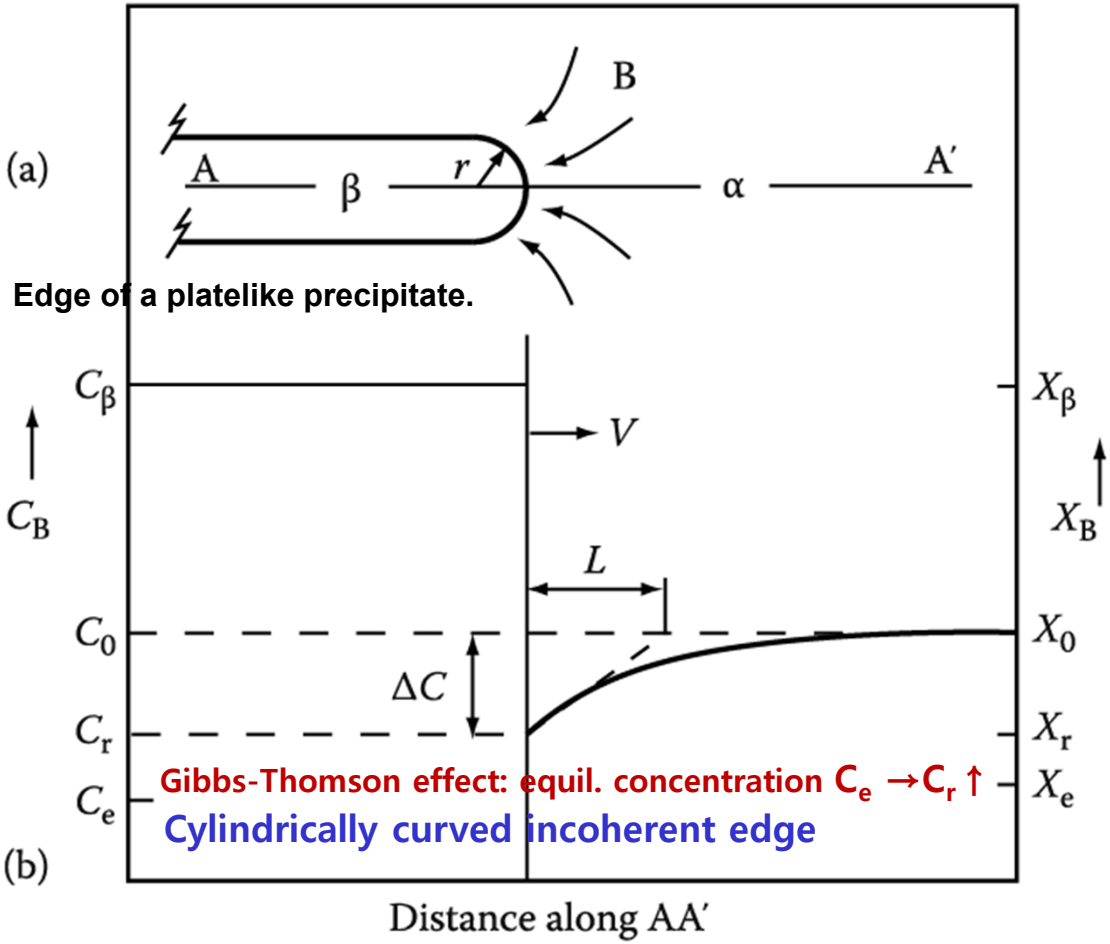

Edge of a platelike precipitate.

Gibbs-Thomson effect: equil. concentration $C_e \rightarrow C_r \uparrow$

Cylindrically curved incoherent edge

Concentration profile along AA' in (a).

From mass conservation,

$$v = \frac{dx}{dt} = \frac{D}{C_\beta - C_e} \cdot \frac{dC}{dx}$$

$$\frac{dC}{dx} = \frac{\Delta C}{L} = \frac{C_0 - C_r}{kr}$$ Radial diffusion

k (const)~1

$$v = \frac{D}{C_\beta - C_r} \cdot \frac{\Delta C}{kr}$$

ΔX for diffusion ∝ edge radius of precipitate

$$X = CV_m \quad \Delta X = \Delta X_0 \left(1 - \frac{r^*}{r}\right)$$

r*=critical radius (if r=r*, ΔX→0)

$$v = \frac{D\Delta X_0}{k(X_\beta - X_r)} \cdot \frac{1}{r}\left(1 - \frac{r^*}{r}\right)$$

$v \rightarrow$ constant $\rightarrow$ $x \propto t$

(If t=2r, v= constant)

Linear growth

Needle → Gibbs-Thomson increase in G = $2\gamma V_m/r$ instead of $\gamma V_m/r$

→ the same equation but the different value of r^*

3) Thickening of Plate-like Precipitates

Thickening of Plate-like Precipitates by Ledge Mechanism

↔ planar incoherent interface with high accommodation factors

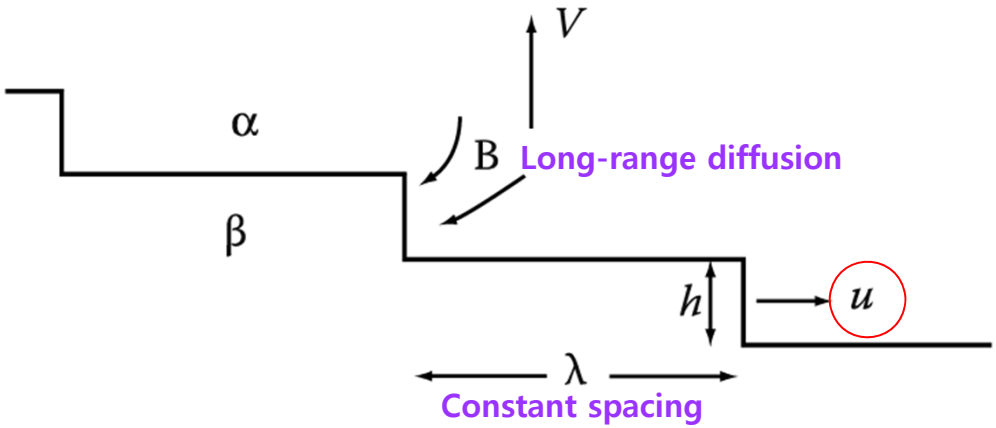

- For the diffusion-controlled growth, a monoatomic-height ledge should be supplied constantly.
- sources of monatomic-height ledge → spiral growth, 2-D nucleation, nucleation at the precipitate edges, or from intersections with other precipitates (heterogeneous 2-D)

Half Thickness Increase

$$v = \frac{uh}{\lambda}$$

u : rate of lateral migration

If the edges of the ledges are incoherent,

Assuming the diffusion-controlled growth,

$$u = \frac{D\Delta X_0}{k(X_\beta - X_e)h}$$

(Here, h= r and $X_r = X_e$, no Gibbs-Thomson effect)

$$v = \frac{uh}{\lambda} \rightarrow v = \frac{D\Delta X_0}{k(X_\beta - X_e)\lambda}$$

$$v = \frac{D}{C_\beta - C_r} \cdot \frac{\Delta C}{kr}$$

very similar to that of plate lengthening

Distance btw ledges

3) Thickening of Plate-like Precipitates

Except spiral growth, supplement of ledge with constant λ is difficult.

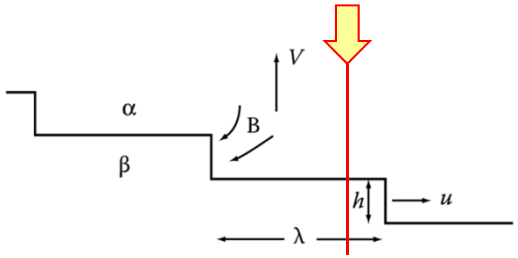

Thickening of γ Plate in the Al-Ag system

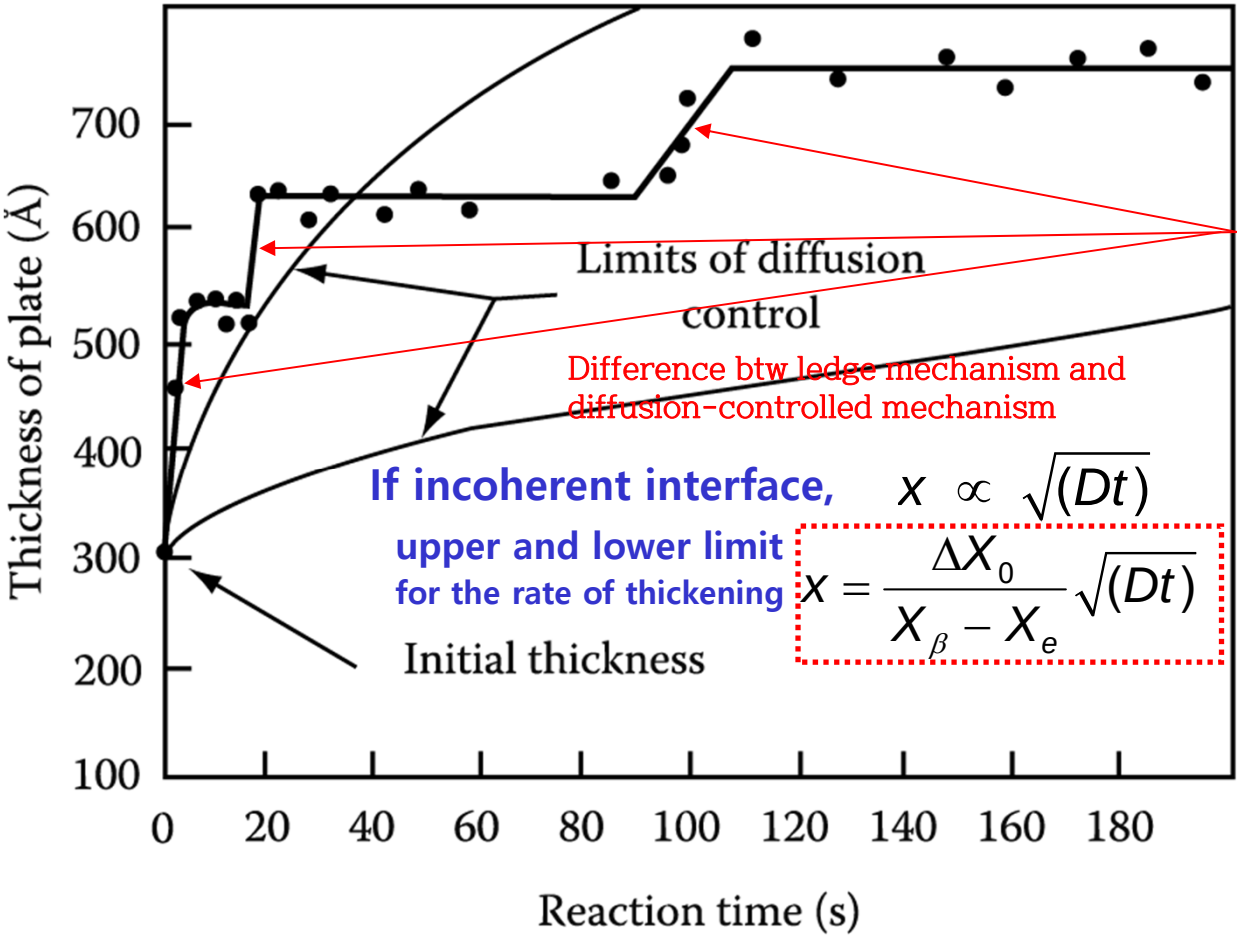

What does this data mean?

appreciable intervals of time
(no perceptible increase in plate thickness)
& thickness increases rapidly as an interfacial ledge passes.

↓

Evidence for the low mobility of semi-coherent interfaces

↓

Thickening rate is not constant

"Ledge nucleation" is rate controlling.

Fig. 5. 22 The thickening of a γ plate in an Al-15 wt% Ag alloy at 400 ℃
measure the thickening rates of individual precipitate plates by using hot-stage TEM.

- **Precipitate growth**

1) Growth behind Planar Incoherent Interfaces

Diffusion-Controlled Thickening:

$$x \propto \sqrt{(Dt)}$$ Parabolic growth

$$v = \frac{D(\Delta C_0)^2}{2(C_\beta - C_e)(C_\beta - C_0)x}$$

$$v \propto \Delta X_0 \propto \sqrt{(D/t)}$$

Supersaturation

2) Diffusion Controlled lengthening of Plates or Needles

Diffusion Controlled lengthening:

$$v = \frac{D\Delta X_0}{k(X_\beta - X_r)} \cdot \frac{1}{r}\left(1 - \frac{r^*}{r}\right)$$

$v \rightarrow$ constant $\rightarrow$ $x \propto t$

Linear growth

3) Thickening of Plate-like Precipitates

Thickening of Plate-like Precipitates by Ledge Mechanism

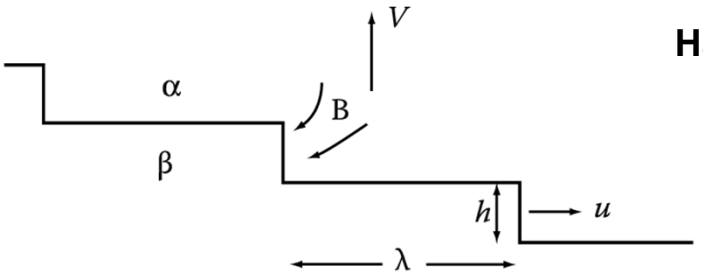

Half Thickness Increase

$$v = \frac{uh}{\lambda} \rightarrow v = \frac{D\Delta X_0}{k(X_\beta - X_e)\lambda}$$

u : rate of lateral migration

Contents for today's class

< Phase Transformation in Solids >

1) Diffusional Transformation (a) Precipitation

Q1: Overall Transformation Kinetics–TTT diagram

"Johnson-Mehl-Avrami Equation"

Q2: Precipitation in Age-Hardening Alloys

Q3: Age Hardening

Q4: How can you design an alloy with high strength at high T?

Q5: Quenched-in vacancies vs Precipitate-free zone

Q1: Overall Transformation Kinetics–TTT diagram

“Johnson-Mehl-Avrami Equation”

5.4 Overall Transformation Kinetics – TTT Diagram

If isothermal transformation,

The fraction of Transformation as a function of Time and Temperature

$\rightarrow$ f(t,T)

Plot f vs log t.

- **isothermal transformation**
- **f ~ volume fraction of β at any time; 0~1**

Plot the fraction of transformation (1%, 99%) in T-log t coordinate.

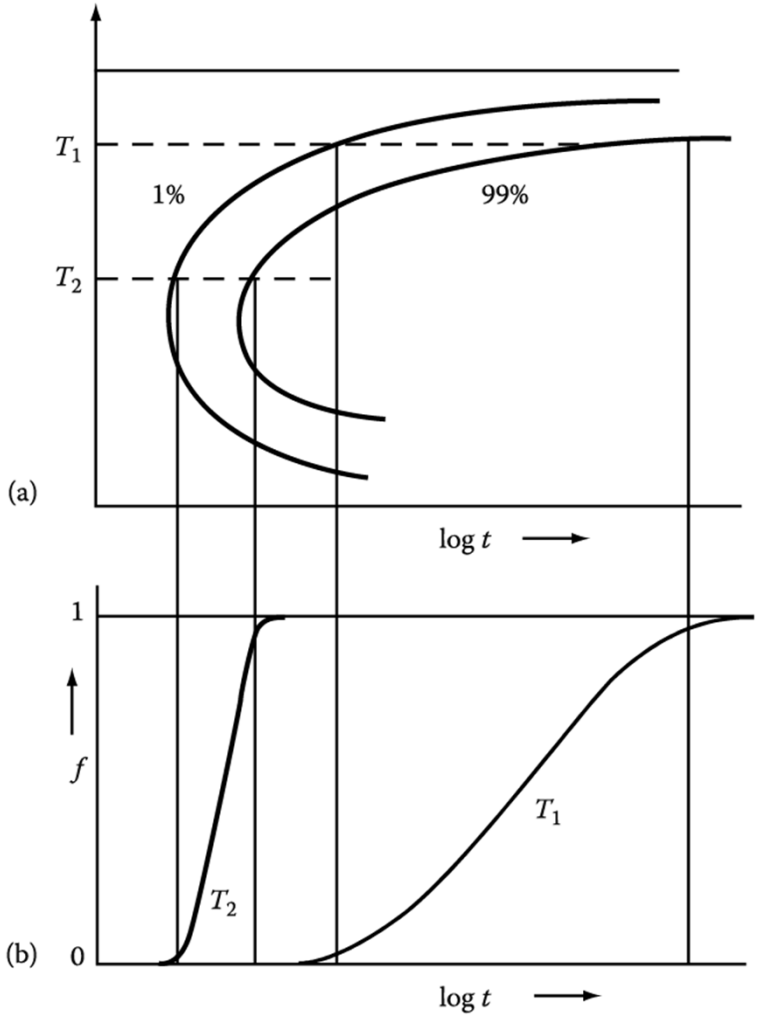

Fig. 5.23 The percentage transformation versus time for different transformation temperatures.

Time–Temperature–Transformation Curves (TTT)

- How much time does it take at any one temperature for a given fraction of the liquid to transform (nucleate and grow) into a crystal?

- $f(t,T) \sim \pi I(T) \mu(T)^3 t^4/3$

  where f is the fractional volume of crystals formed, typically taken to be 10^{-6}, a barely observable crystal volume.

Nucleation rates

$$I = n\nu \exp\left\{\left(\frac{16\pi\Delta H_{cryst}}{81RT}\right)\left(\frac{T_m}{\Delta T}\right)^2\right\}\exp\left\{\frac{-\Delta E_D}{RT}\right\}$$

Growth rates

$$\mu(T) = \left(\frac{fRT}{3N\pi a^2 \eta(T)}\right)\left(1-\exp\left[\left(\frac{\Delta H_m}{RT}\right)\left(\frac{\Delta T}{T_m}\right)\right]\right)$$

Nucleation and Growth Rates – Poor Glass Formers

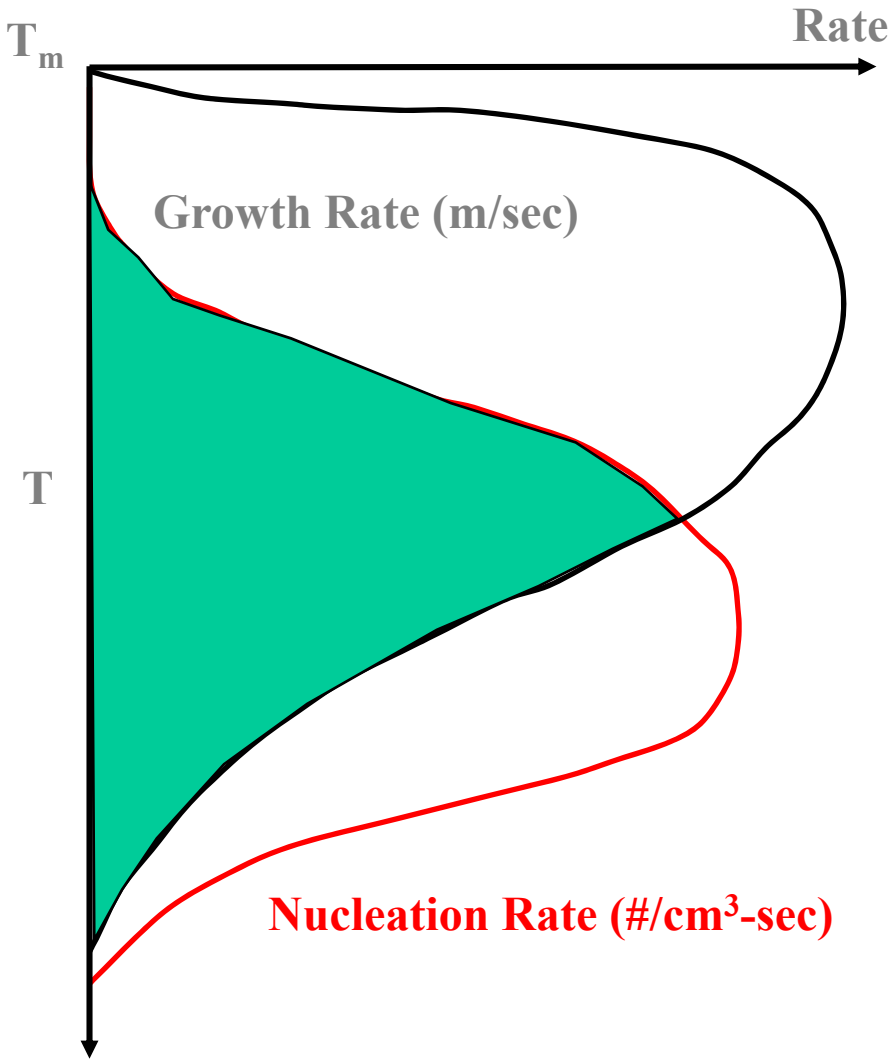

- **Strong overlap of growth and nucleation rates**
- **Nucleation rate is high**
- **Growth rate is high**
- **Both are high at the same temperature**

Nucleation and Growth Rates – Good Glass Formers

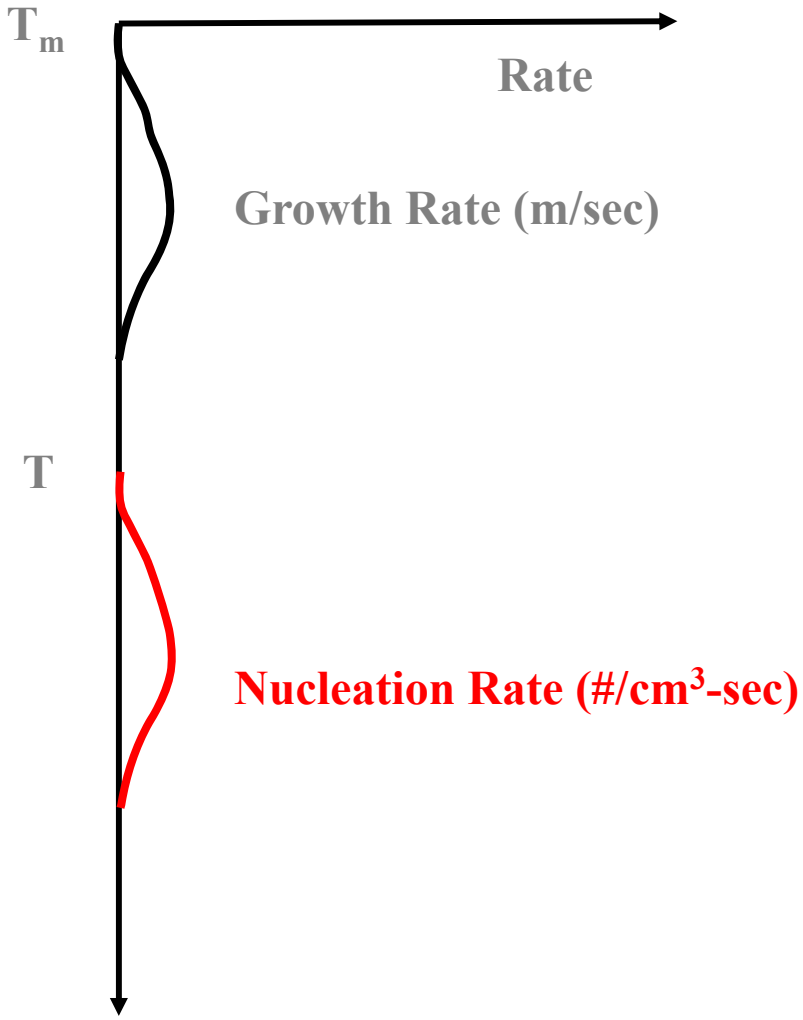

- **No overlap of growth and nucleation rates**
- Nucleation rate is small
- Growth rate is small
- At any one temperature one of the two is zero

* Time-Temperature-Transformation diagrams

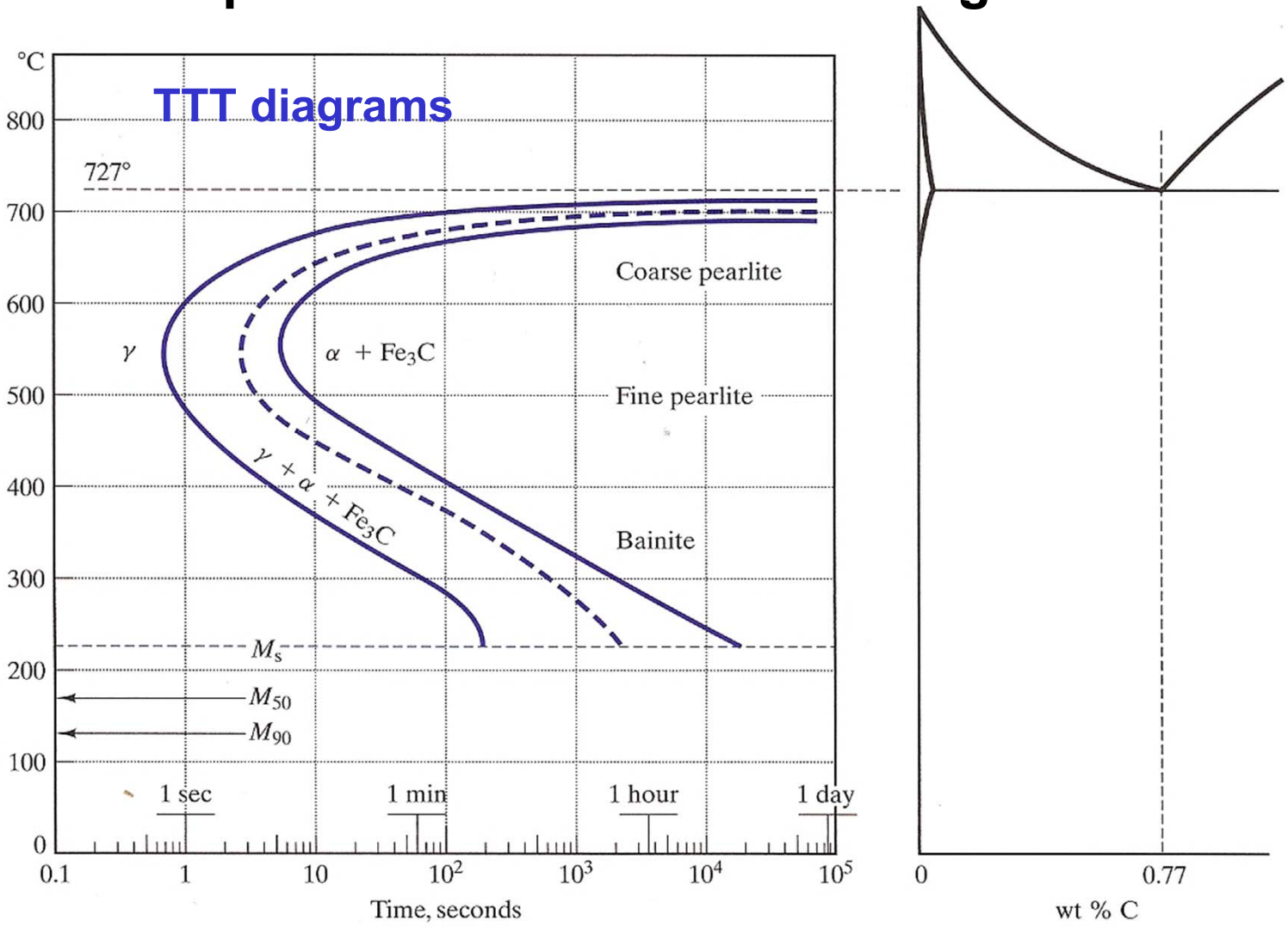

FIGURE 10.11 *A more complete TTT diagram for eutectoid steel than was given in Figure 10.7. The various stages of the time-independent (or diffusionless) martensitic transformation are shown as horizontal lines. M_s represents the start, M_{50} represents 50% transformation, and M_{90} represents 90% transformation. One hundred percent transformation to martensite is not complete until a final temperature (M_f) of −46°C.*

* Continuous Cooling Transformation diagrams

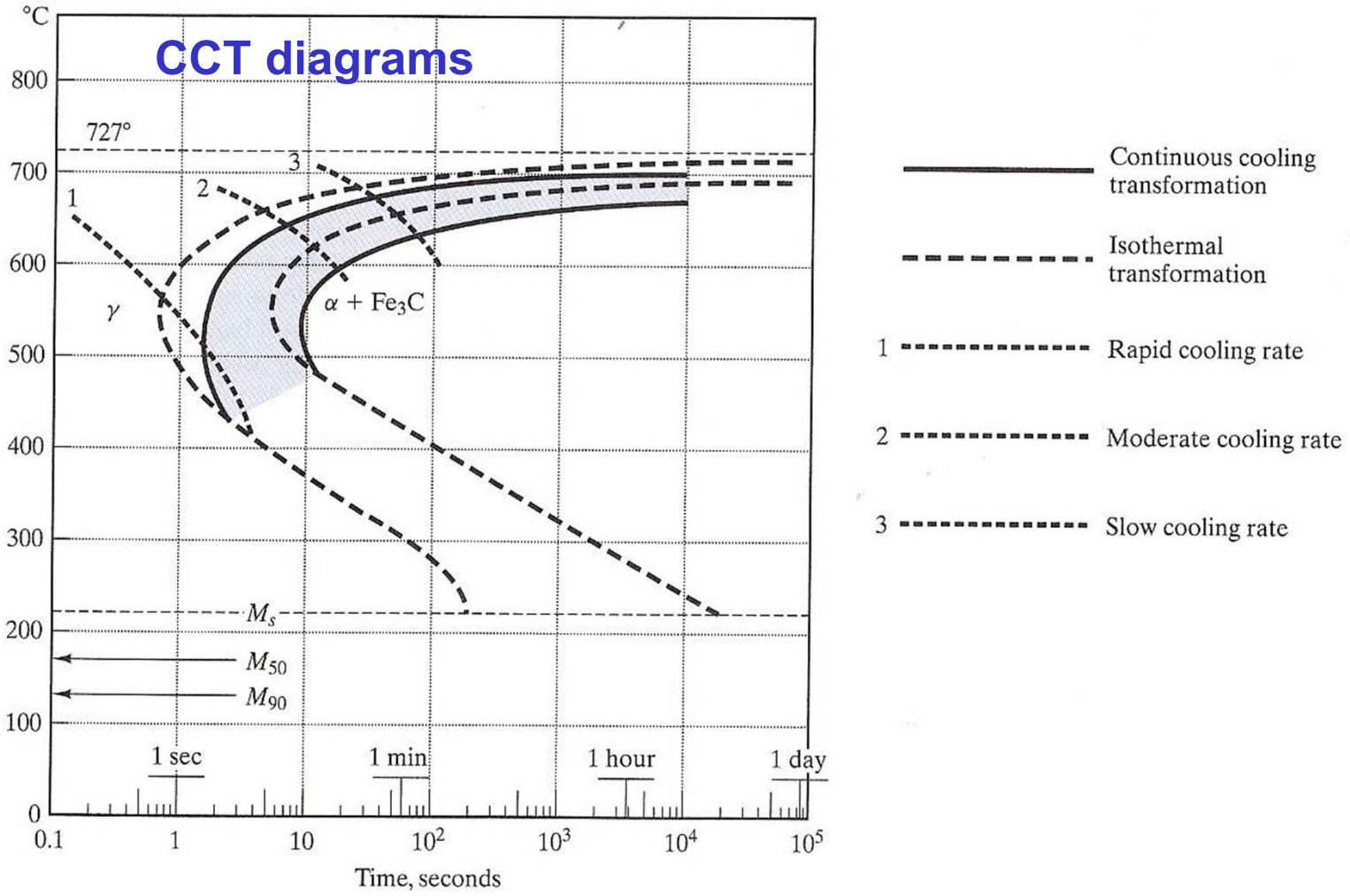

FIGURE 10.14 *A continuous cooling transformation (CCT) diagram is shown superimposed on the isothermal transformation diagram of Figure 10.11. The general effect of continuous cooling is to shift the transformation curves downward and toward the right. (After* Atlas of Isothermal Transformation and Cooling Transformation Diagrams, *American Society for Metals, Metals Park, OH, 1977.)*

Influence factors for $f(t,T)$: nucleation rate, growth rate, density and distribution of nucleation sites, impingement of adjacent cells

Example,

Three Transformation Types

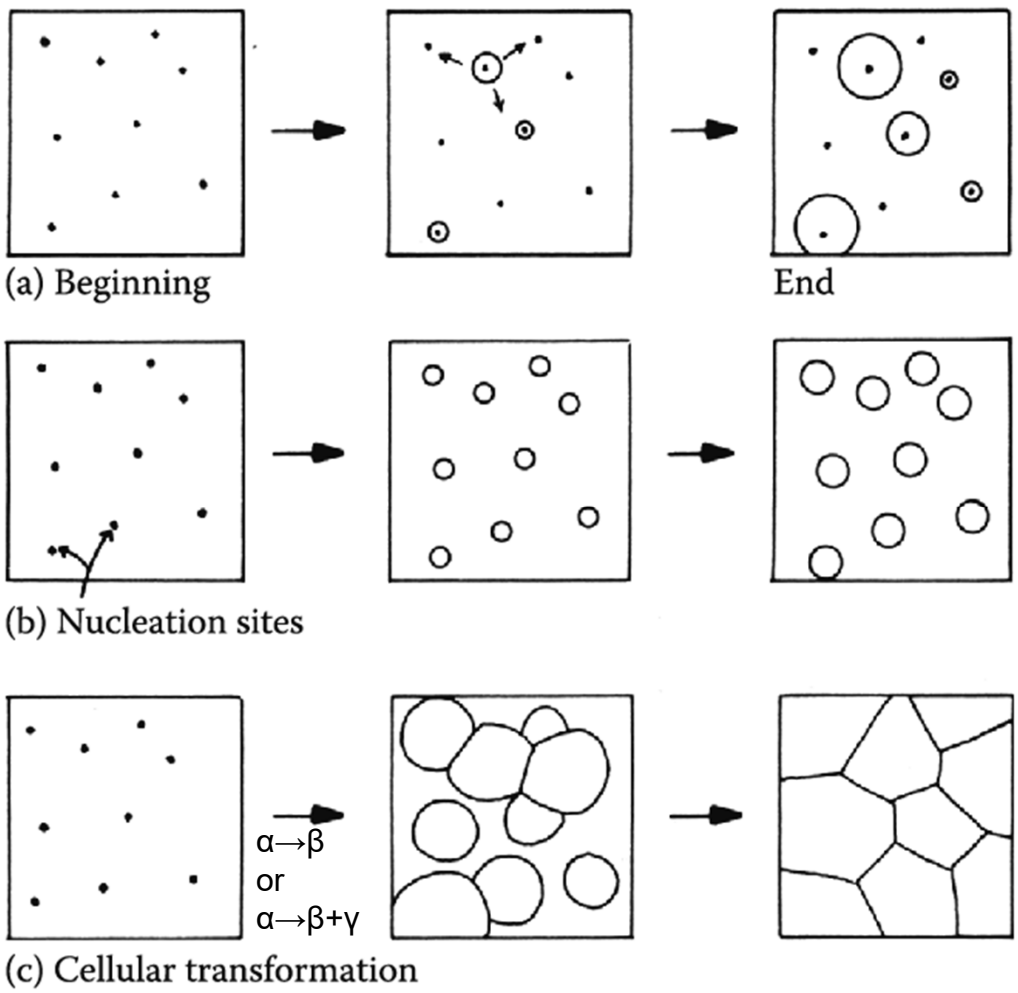

Fig. 5.24 (a) Nucleation at a constant rate during the whole transformation.
(b) Site saturation – all nucleation occurs at the beginning of transformation.
(c) A cellular transformation.

Wide range of particle sizes

(a) continuous nucleation

Metastable α phase with many nucleation sites by quenching to T_t

→ ***f* depends on the *nucleation rate and the growth rate.***

(b) all nuclei present at t = 0

→ ***f* depends on the *number of nucleation sites and the growth rate.***

(c) All of the parent phase is consumed by the transformation product.

Transformation terminate by the impingement of adjacent cells growing with a constant velocity.

→ **pearlite, cellular ppt, massive transformation, recrystallization**

α → β

Transformation Kinetics

- **Avrami proposed that for a three-dimensional nucleation and growth process kinetic law**

$$f = 1 - \exp\left(-kt^n\right)$$ Johnson-Mehl-Avrami equation

f : volume fraction transformed $= \dfrac{\text{Volume of new phase}}{\text{Volume of specimen}}$

- **Assumption :**
  - √ reaction produces by nucleation and growth
  - √ nucleation occurs randomly throughout specimen
  - √ reaction product grows rapidly until impingement

Constant Nucleation Rate Conditions

- **Nucleation rate (*I*) is constant.**
- **Growth rate (v) is constant.**
- **No compositional change**

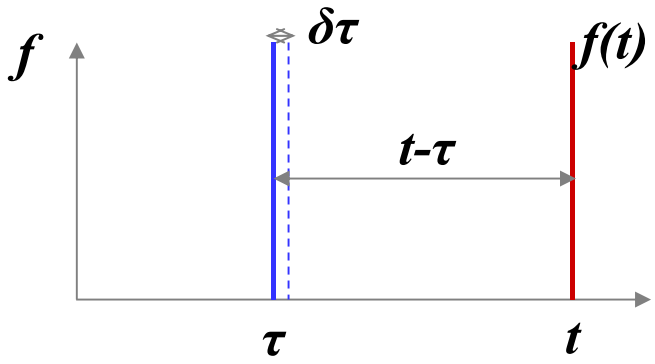

$$df_e = \frac{\left(\begin{array}{l}\text{Vol. of one particle nucleated}\\ \text{during } d\tau \text{ measured at time t}\end{array}\right)\times\left(\begin{array}{l}\text{number of nuclei}\\ \text{formed during } d\tau\end{array}\right)}{\text{Volume of specimen}}$$

$$df_e = \frac{\frac{4}{3}\pi\left[v(t-\tau)\right]^3 \times (IV_0 d\tau)}{V_0}$$

$$f_e(t) = \int_o^t I \cdot \frac{4}{3}\pi\left[v(t-\tau)\right]^3 d\tau$$

$$= I \cdot \frac{4}{3}\pi v^3 \left[-\frac{1}{4}(t-\tau)^4\right]_0^t = \frac{1}{3}\pi I v^3 t^4$$

$$V = \frac{4}{3}\pi r^3 = \frac{4}{3}\pi (vt)^3$$

$$V' = \frac{4}{3}\pi v^3 (t-\tau)^3$$

- do not consider impingement & repeated nucleation
- only true for $f \ll 1$

As time passes the β cells will eventually impinge on one another and the rate of transformation will decrease again.

Constant Nucleation Rate Conditions

- consider impingement + repeated nucleation effects

$$df = (1-f)\,df_e \longrightarrow df_e = \frac{df}{1-f}$$

$$f_e = -\ln(1-f)$$

$$f(t) = 1-\exp(-f_e(t)) = 1-\exp\left(-\frac{\pi}{3} I v^3 t^4\right)$$

* Short time:
1-exp(z)~Z (z ≪1)

* Long time:
t→∞, f →1

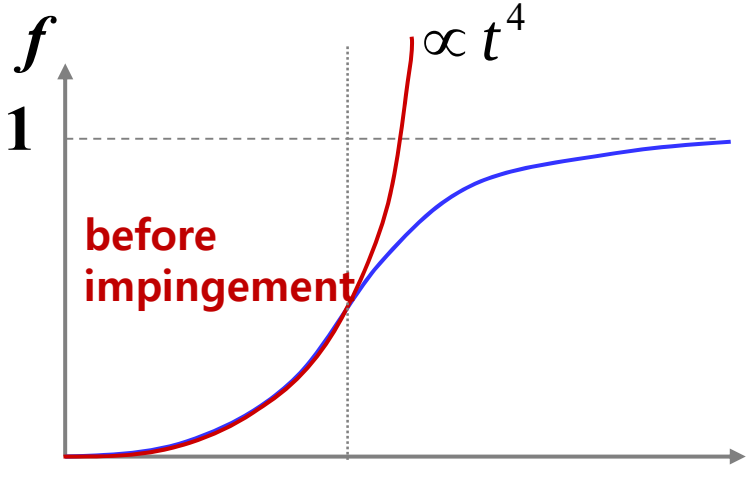

Johnson-Mehl-Avrami Equation

$$f = 1-\exp(-kt^n)$$

k: T sensitive $f(I, v)$ $\quad -\frac{\pi}{3} I v^3$

n: 1 ~ 4 (depend on nucleation mecnanism)

Growth controlled. Nucleation-controlled.

If no change of nucleation mechanism during phase transformation, n is not related to T.

i.e. 50% transform

Exp (-0.7) = 0.5

$$kt_{0.5}^n = 0.7 \quad t_{0.5} = \frac{0.7}{k^{1/n}} \xrightarrow{\frac{\pi}{3} I v^3} t_{0.5} = \frac{0.9}{N^{1/4} v^{3/4}}$$

Rapid transformations are associated with (large values of k), or (rapid nucleation and growth rates)

5.4 Overall Transformation Kinetics

If isothermal transformation,

The fraction of Transformation as a function of Time and Temp. → $f(t,T)$

TTT Diagram ⟺ CCT Diagram

* Constant Nucleation Rate Conditions

$$f(t) = 1 - \exp\left(-f_e(t)\right) = 1 - \exp\left(-\frac{\pi}{3} I v^3 t^4\right)$$

* Short time:
1-exp(z)~Z (z ≪1)

* Long time:
t→∞, f →1

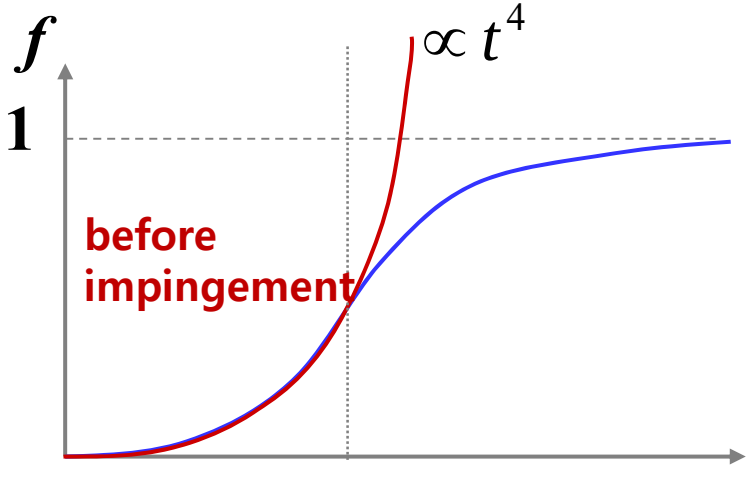

Johnson-Mehl-Avrami Equation

$$f = 1 - \exp\left(-kt^n\right)$$

$-\frac{\pi}{3} I v^3$

k: *T* sensitive ***f(I, v)***

n: **1 ~ 4 (depend on nucleation mecnanism)**

Growth controlled. **Nucleation-controlled.**

If no change of nucleation mechanism during phase transformation, n is not related to T.

i.e. 50% transform

Exp (-0.7) = 0.5

$$kt_{0.5}^n = 0.7 \quad t_{0.5} = \frac{0.7}{k^{1/n}} \xrightarrow{\frac{\pi}{3} I v^3} t_{0.5} = \frac{0.9}{I^{1/4} v^{3/4}}$$

Rapid transformations are associated with (large values of k), or (rapid nucleation and growth rates)

Q2: Precipitation in Age-Hardening Alloys

The theory of nucleation and growth can provide general guidelines for understanding civilian transformation.

5.5 Precipitation in Age-Hardening Alloys

Table 5.2 Some precipitation-Hardening Sequences

Base Metal	Alloy	Precipitation Sequence
Aluminum	Al–Ag	GPZ (spheres) $\rightarrow \gamma'$ (plates) $\rightarrow \gamma$ (Ag_2Al)
	Al–Cu	GPZ (disks) $\rightarrow \theta''$ (disks) $\rightarrow \theta'$ (plates) $\rightarrow \theta$ ($CuAl_2$)
	Al–Cu–Mg	GPZ (rods) $\rightarrow S'$ (laths) $\rightarrow S$ ($CuMgAl_2$) (laths)
	Al–Zn–Mg	GPZ (spheres) $\rightarrow \eta'$ (plates) $\rightarrow \eta$ ($MgZn_2$) (plates or rods)
	Al–Mg–Si	GPZ (rods) $\rightarrow \beta'$ (rods) $\rightarrow \beta$ (Mg_2Si) (plates)
Copper	Cu–Be	GPZ (disks) $\rightarrow \gamma' \rightarrow \gamma$ (CuBe)
	Cu–Co	GPZ (spheres) $\rightarrow \beta$ (Co) (plates)
Iron	Fe–C	ε-carbide (disks) $\rightarrow Fe_3C$ (plates)
	Fe–N	α'' (disks) $\rightarrow Fe_4N$
Nickel	Ni–Cr–Ti–Al	γ' (cubes or spheres)

Source: Mainly from Martin, J.W., in *Precipitation Hardening*, Pergamon Press, Oxford, 1968.

Let us now turn to a consideration of some examples of the great variety of civilian transformations in solid.

5.5 Precipitation in Age-Hardening Alloys

Precipitation in Aluminum-Copper Alloys

Al-4 wt%Cu (1.7 at %)

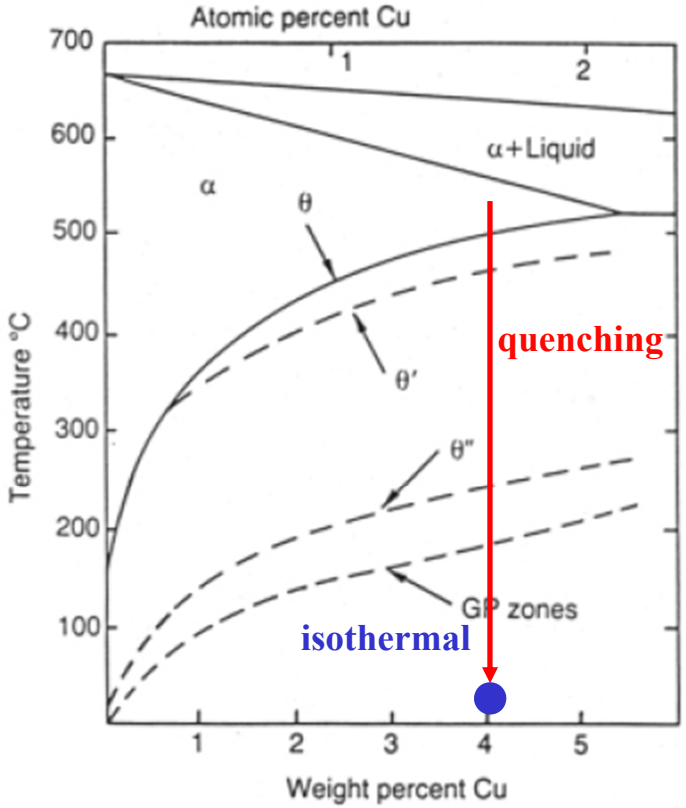

α_0 **540°C heat treatment →**
Quenching + Isothermal (below 180°C)

Supersaturated solid solution

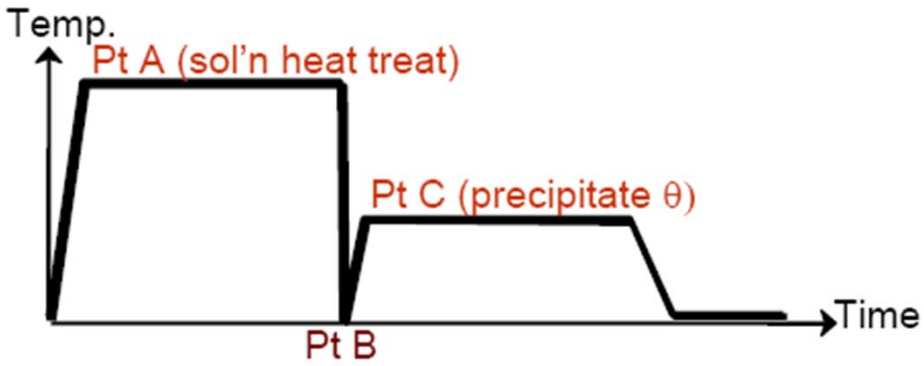

$\rightarrow \alpha_1$ **+GP zones**

$\rightarrow \alpha_2 + \theta'' \rightarrow \alpha_3 + \theta' \rightarrow \alpha_4 + \theta$

$(CuAl_2)$

Fig. 5.25 Al-Cu phase diagram showing the metastable GP zone, Θ″ and Θ′ solvuses. (Reproduced from G. Lorimer, *Precipitation Processes in Solids*, K.C. Russell and H.I. Aaronson (Eds.), The Metallurgical Society of AMIE, 1978, p. 87.)

In most system, α, β phase~ different crystal structure → incoherent nuclei with large γ ~ impossible to homogeneous nucleation of β → Homogeneous nucleation of metastable phase β′ (GP Zones, Section 5.5.1)

Driving force for GP zone precipitation

5.5.1 GP Zones

$$\Delta G_{\theta}^{*} > (\Delta G_V - \Delta G_s) >> \Delta G_{zone}^{*}$$

The zones minimize their strain energy by choosing a disc-shape perpendicular to the elastically soft <100> directions in the fcc matrix (as shown in Fig. 5.26).

2 atomic layers thick and 10 nm in diameter with a spacing of ~10 nm

Fully coherent Cu-rich area with very low interfacial E

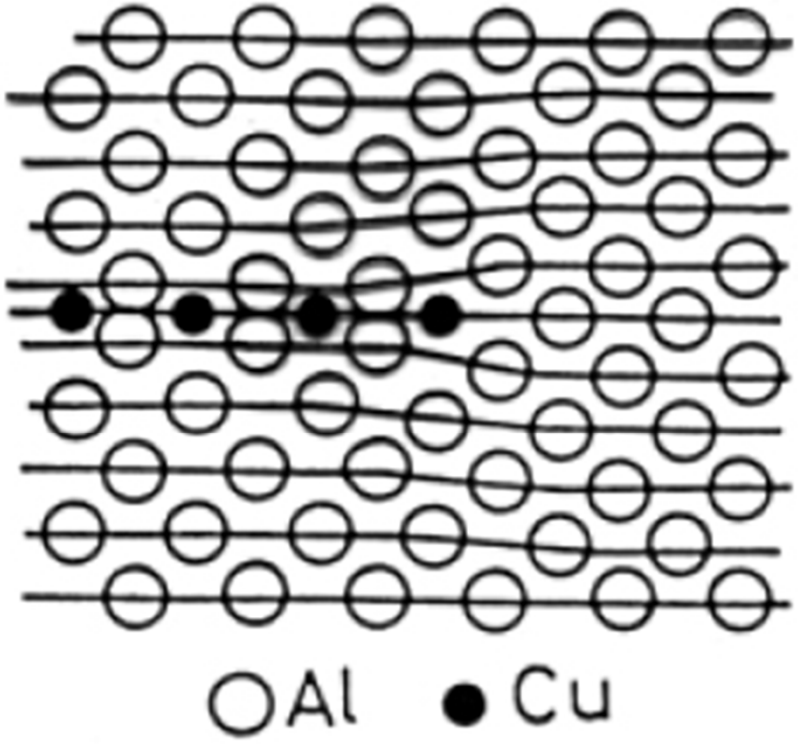

Fig. 5.26 Section through a GP zone parallel to the (200) plane. (Based on the work of V. Gerold: *Zeitschrift für Metallkunde* **45** (1954) 599.)

: 이러한 응집체는 완전한 석출 입자로 볼 수 없으며, 때때로 석출대 (zone)로 명명함.

The zone appear to be homogeneously nucleated, however, excess vacancies are thought to play an important role in their formation (be returned to later)

GP zones of Al-Cu alloys (x 720,000, TEM)

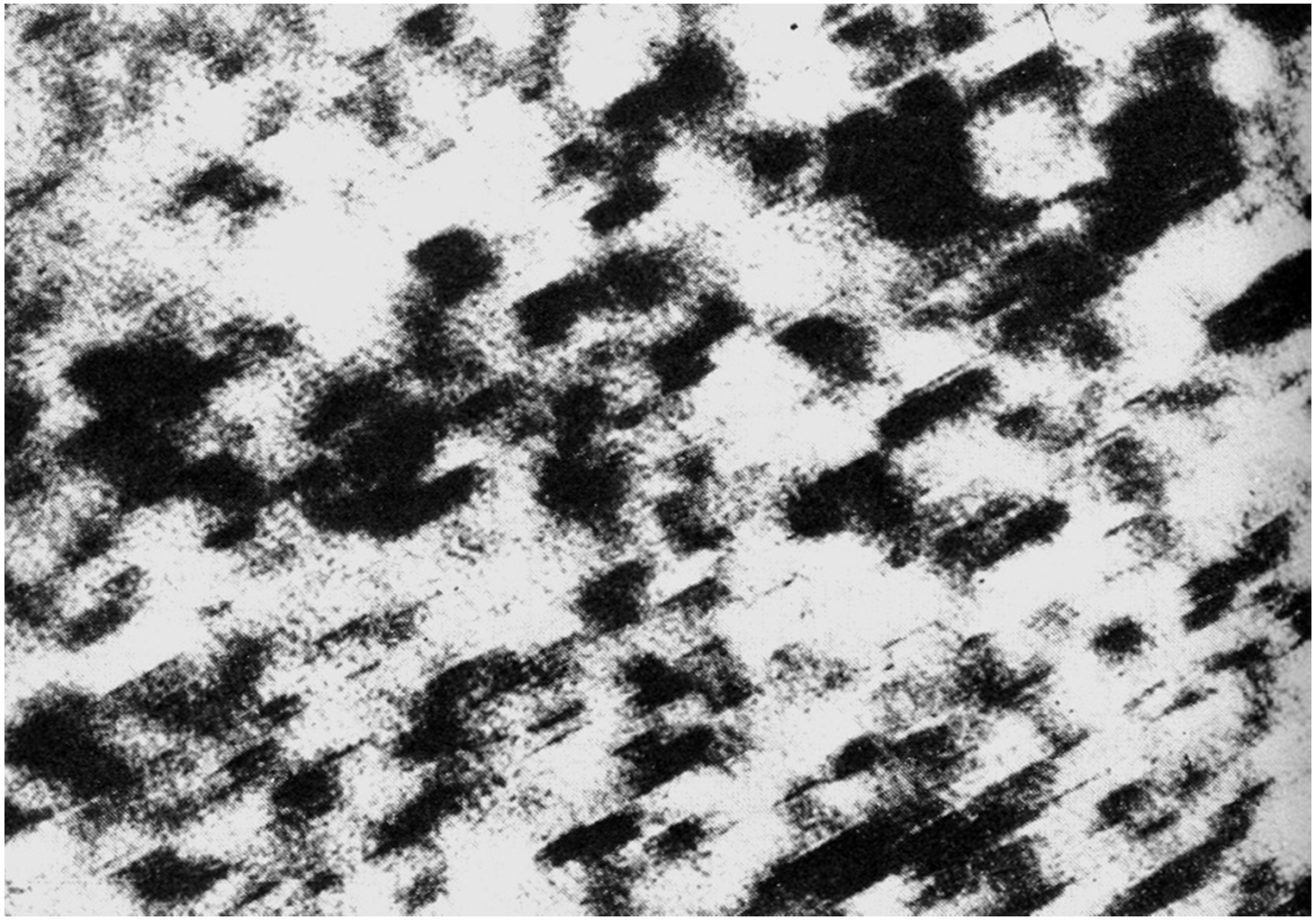

Fully coherent, about 2 atomic layers thick and
10 nm in diameter with a spacing of ~ 10 nm

: The contrast in the image is due to the coherency misfit strain perpendicular to the zones.
(Coherency misfit strain→local variations in the intensity of electron diffraction→image contrast change)

Transition phases

$\alpha_0 \rightarrow \alpha_1$+GP zone$\rightarrow\alpha_2$+$\theta''$ $\rightarrow\alpha_3$+θ' $\rightarrow\alpha_4$+θ ($CuAl_2$)

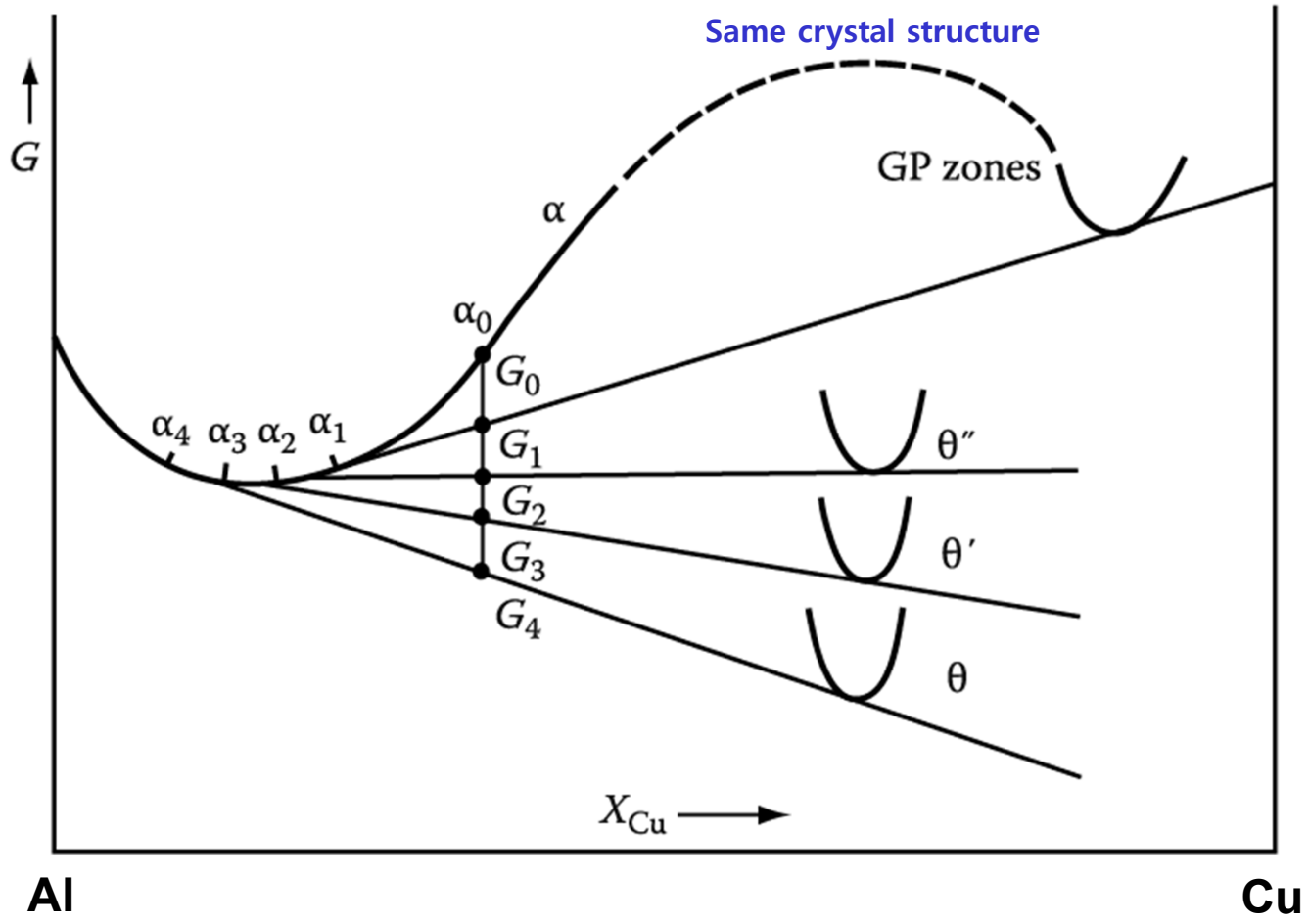

Fig. 5.27 A schematic molar free energy diagram for the Al-Cu system.

$\alpha_0 \rightarrow \alpha_1$+GP zone$\rightarrow\alpha_2+\theta'' \rightarrow\alpha_3+\theta' \rightarrow\alpha_4+\theta$ ($CuAl_2$)

Low Activation Energy of Transition Phases

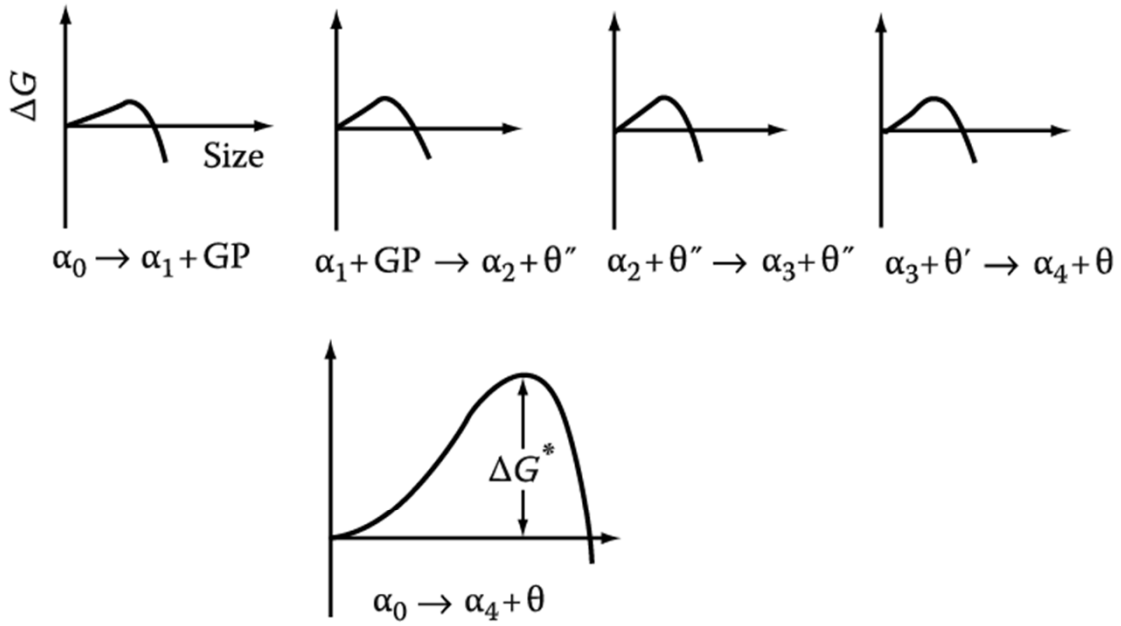

∵ the crystal structures of the transition phases are intermediate between those of the matrix and the equilibrium phase.

Transition phases (중간상, θ″ & θ′): a high degree of coherence, low interfacial E contribution to min ΔG*.

Equilibrium phase (평형상, θ): complex crystal structure that is incompatible with the matrix → high E interfaces and high ΔG*.

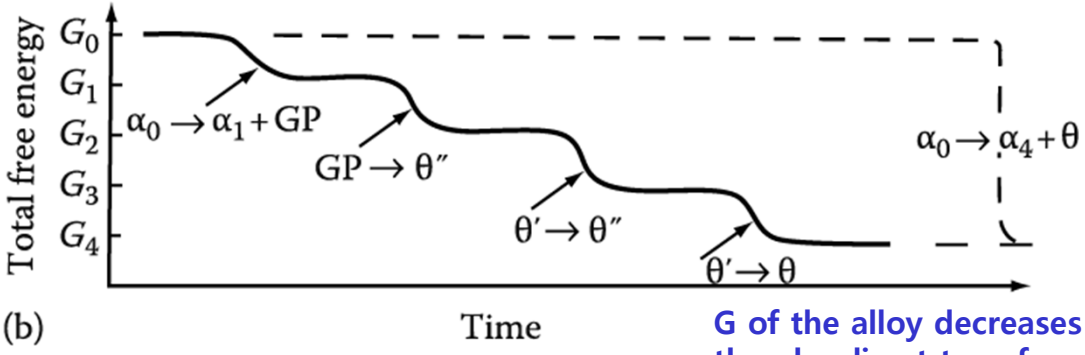

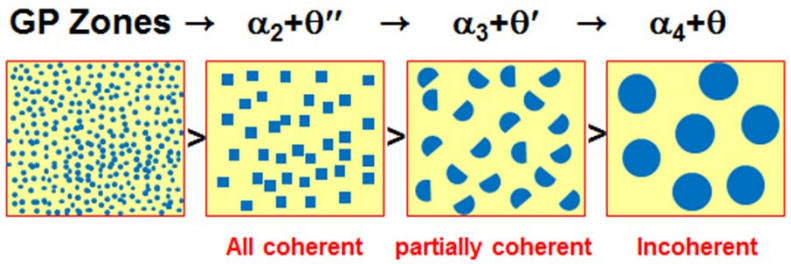

G of the alloy decreases more rapidly via the transition phases than by direct transformation to the equilibrium phase.

(a) The activation E barrier to the formation of each transition phase is very small in comparison to the barrier against the direct precipitation of the equilibrium phase. (b) Schematic diagram showing the total free E of the alloy versus time.

The Crystal Structures of θ″, θ′ and θ

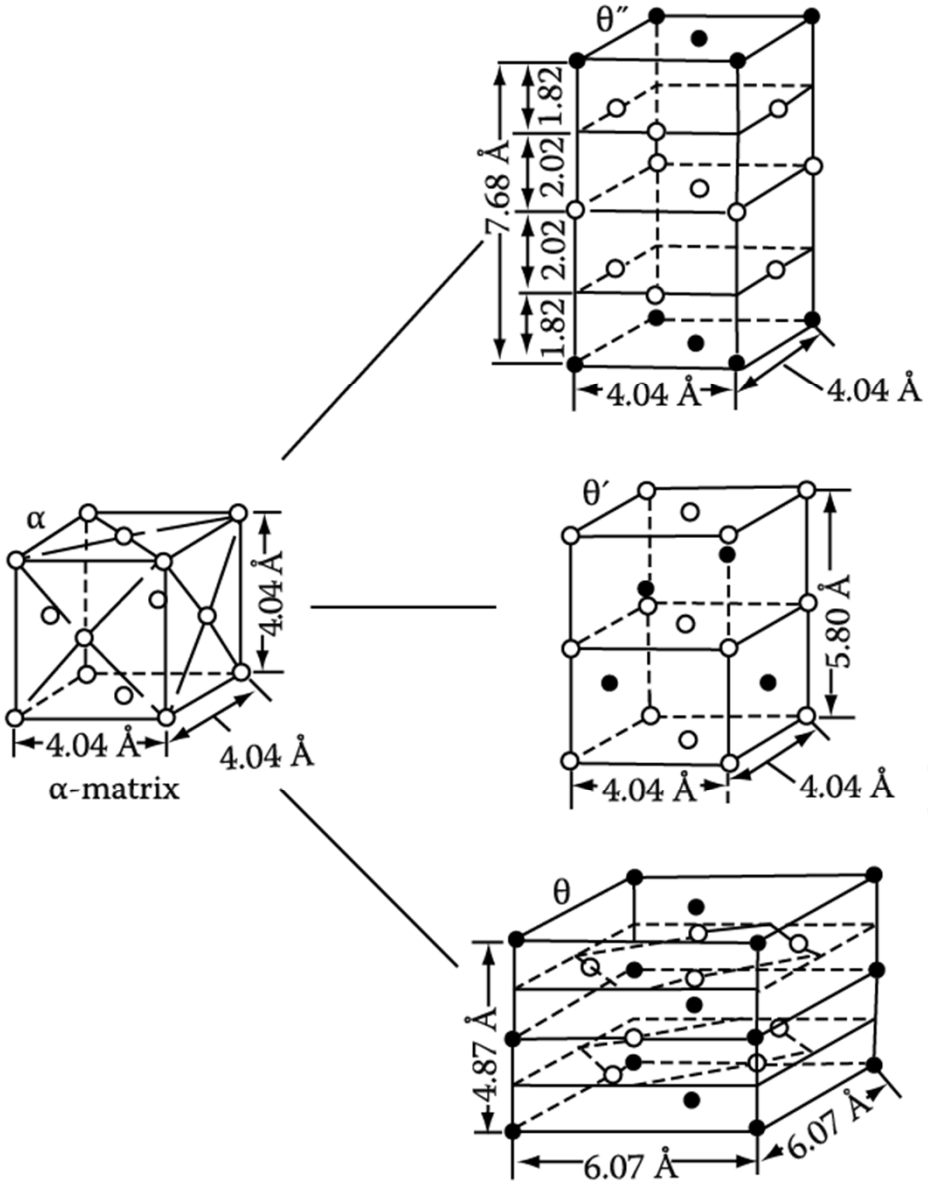

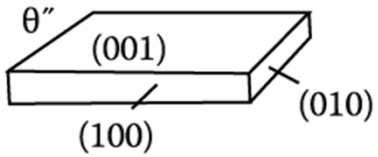

All sides coherent

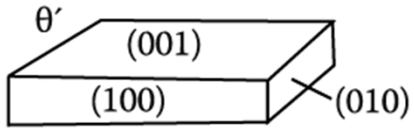

(001) Coherent or semicoherent

(100) } Not coherent
(010) }

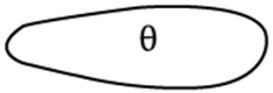

Incoherent

A tetragonal unit cell (= a distorted fcc structure in which the Cu and Al atoms are ordered on (001) planes.)

& a small distortion in the [001] direction of (010) and (100) faces

A tetragonal with an approximate composition $CuAl_2$

Different crystal structure in (010) and (100) faces to the matrix and a large misfit in the [001] direction

Approximate composition $CuAl_2$ and complex BCT structure

Fig. 5.29 Structure and morphology of θ'', θ' and θ in Al-Cu (○ Al. ● Cu).

θ″ of Al-Cu alloys (x 63,000, TEM)

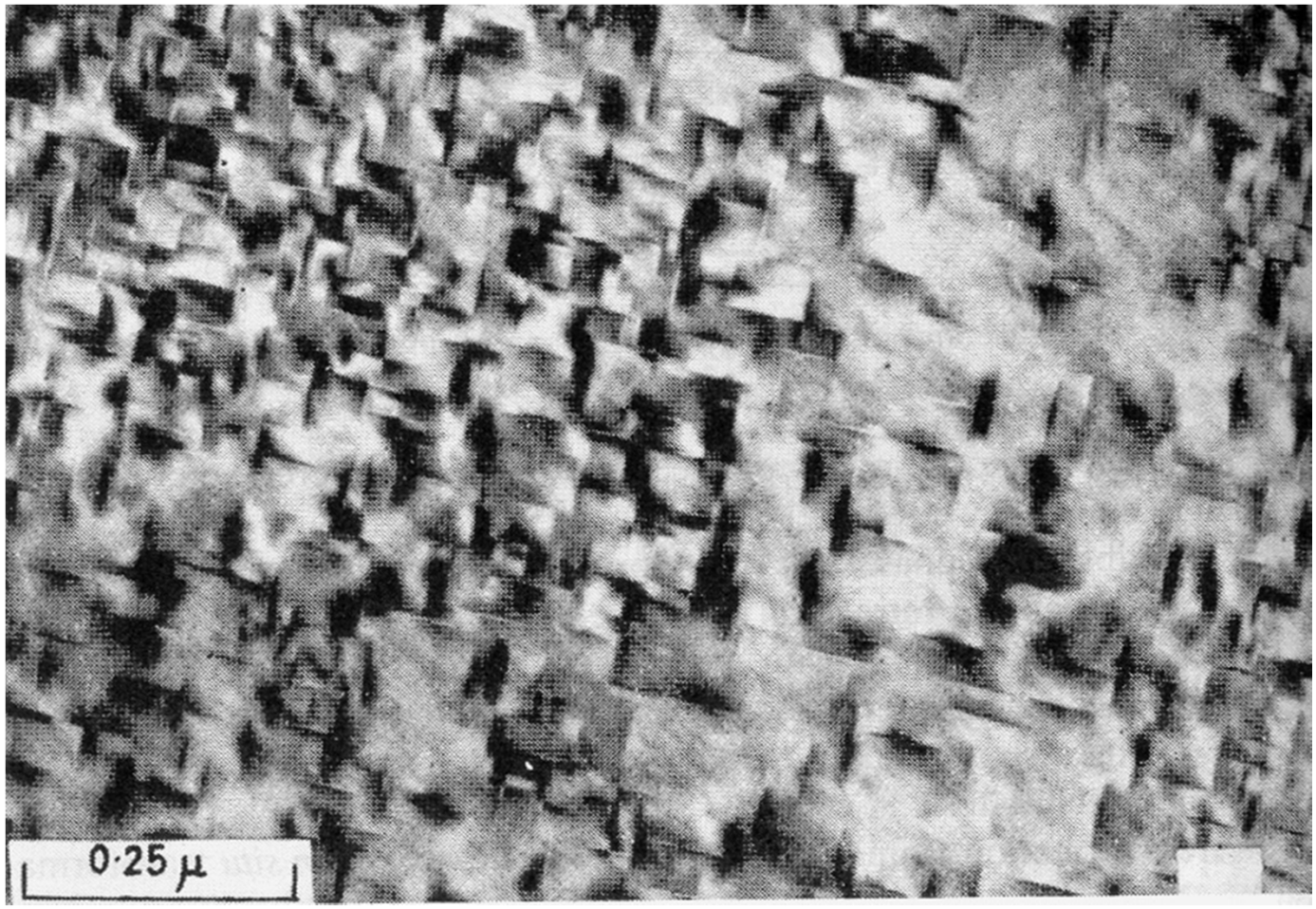

Tetragonal unit cell, essentially a distorted fcc in which Cu and Al atoms are ordered on (001) planes, fully-coherent plate-like ppt with $\{001\}_\alpha$ habit plane. ~ 10 nm thick and 100 nm in diameter (larger than GP zones).

: Like the GP zones, the θ″ precipitates are visible by virtue of the coherency-strain fields caused by the misfit perpendicular to the plates.

θ′ of Al-Cu alloys (x 18,000, TEM)

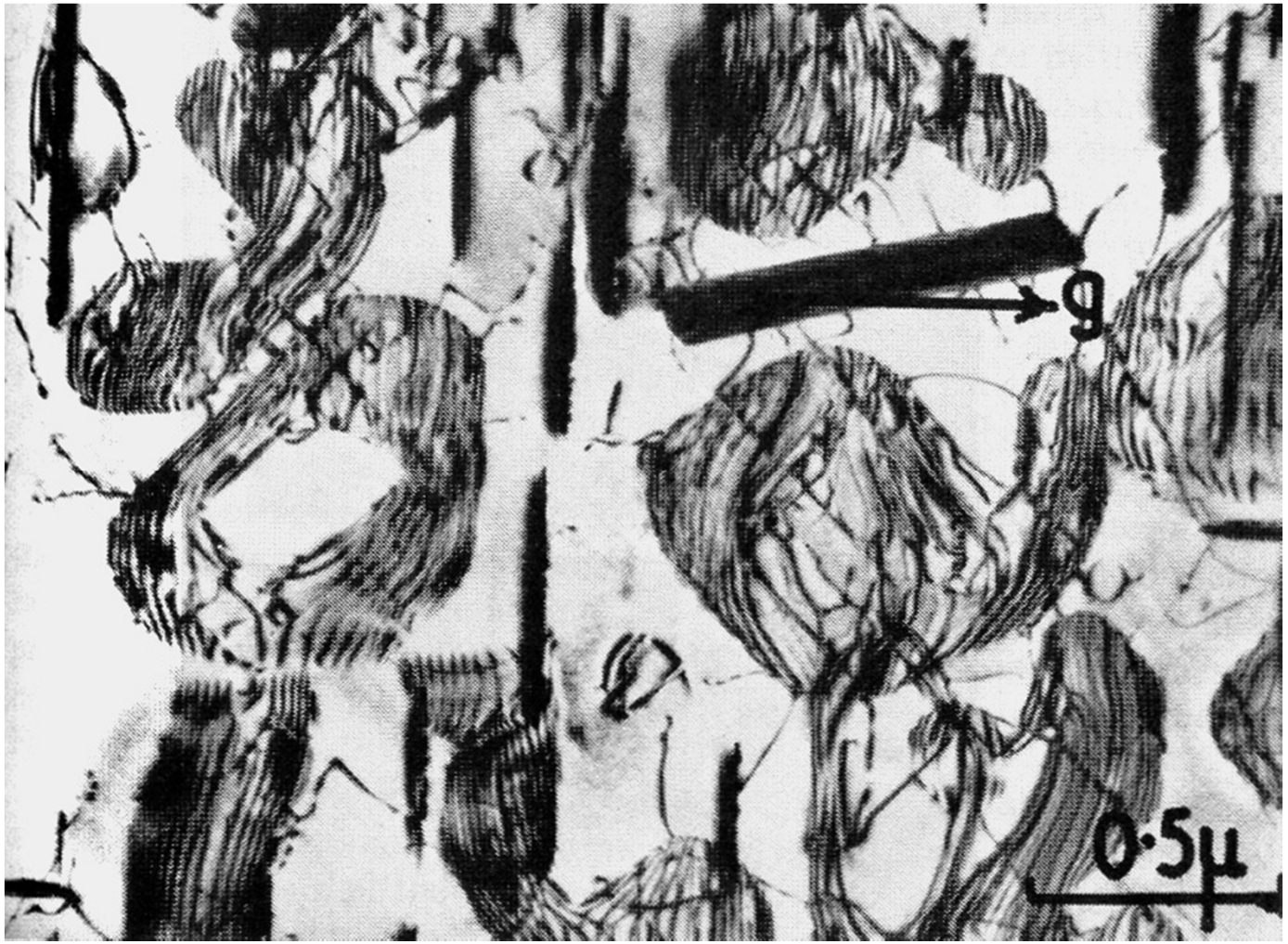

θ′ has (001) planes that are identical with $\{001\}_\alpha$ and forms as plates on $\{001\}_\alpha$ with the same orientation relationship as θ″.
But, (100), (010) planes → incoherent, ~ 1 μm in diameter.

: The broad faces of the plates are initially fully coherent but lose coherency as the plates grow, while the edges of the plates are either incoherent or have a complex semicoherent structure.

θ of Al-Cu alloys x 8,000

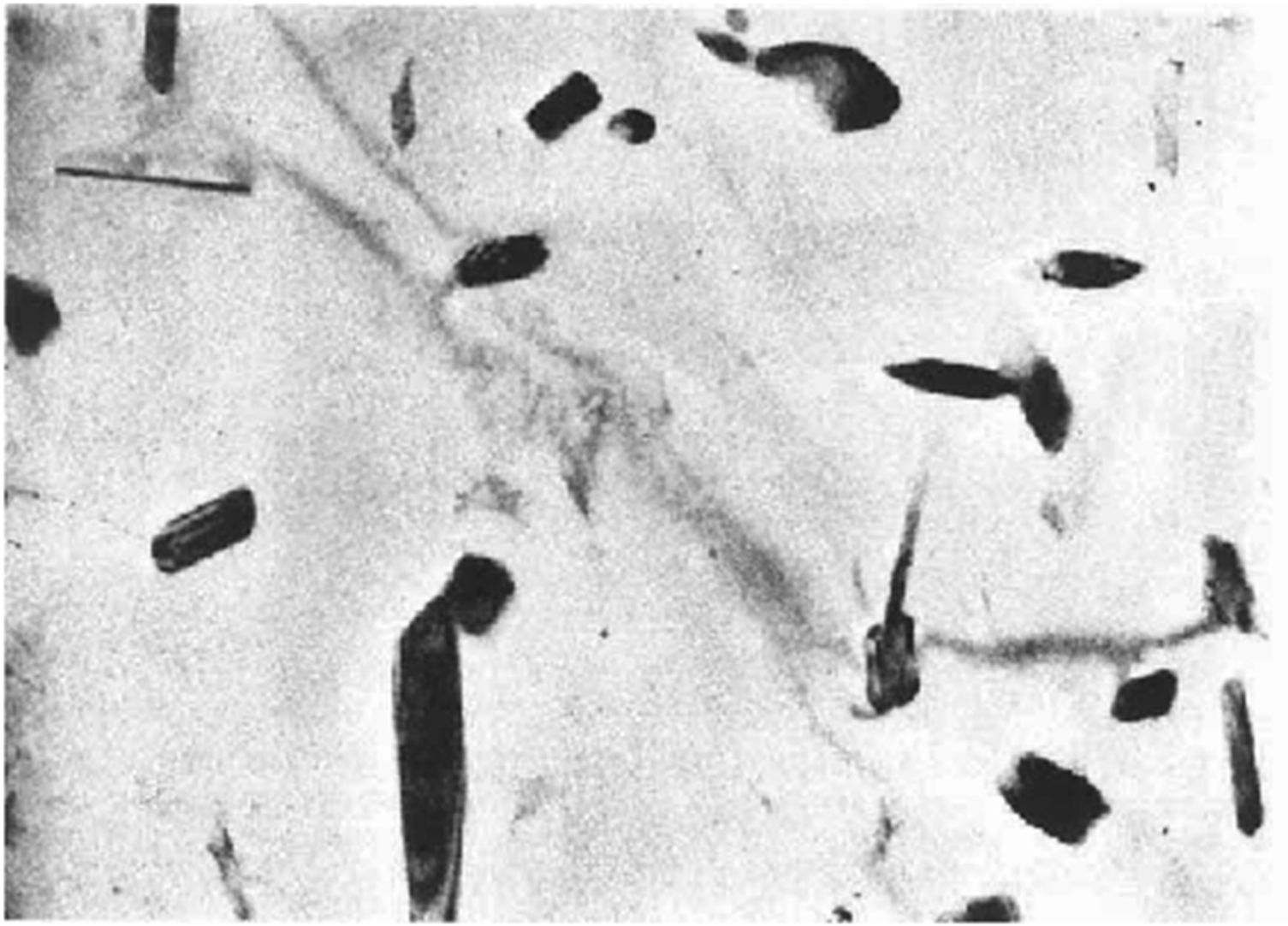

$CuAl_2$: complex body centered tetragonal, incoherent or complex semicoherent

: large size and coarse distribution of the precipitates

Nucleation sites
in Al-Cu alloys

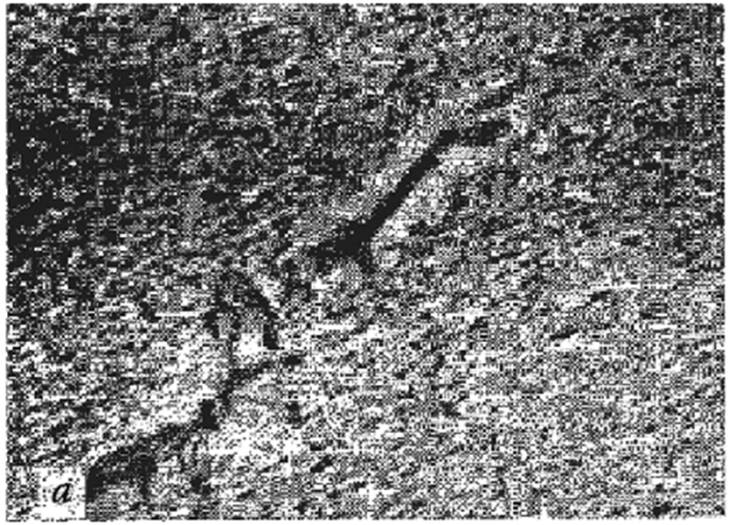

(a) θ" → θ'. θ' nucleates at dislocation (x 70,000).

: Dislocation can reduce the misfit in two <100> matrix directions.

As the θ' grows the surrounding, less-stable θ" phase can be seen to dissolve.

(0) GP zones → θ":

GP zones

~ very potent nucleation sites for θ"

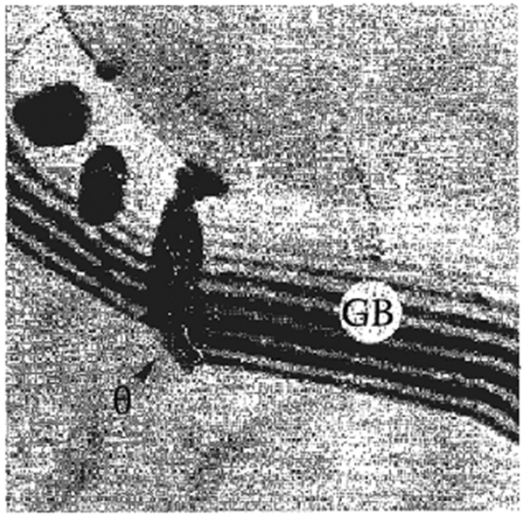

(b) θ nucleation on grain boundary (GB)(x 56,000)

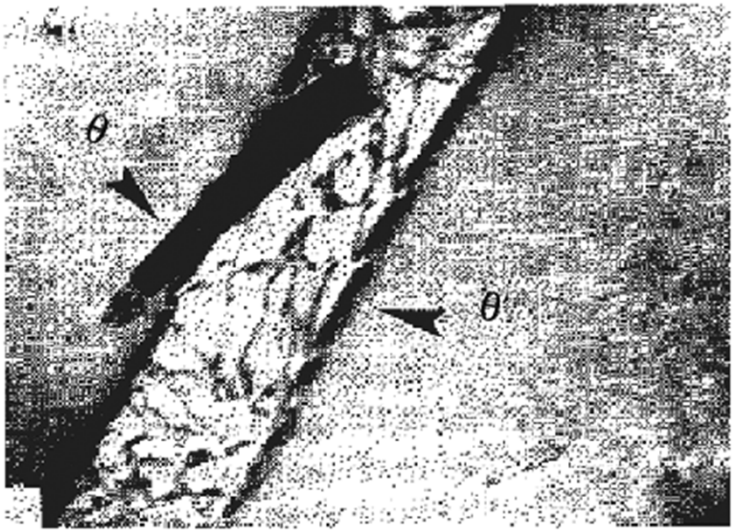

(c) θ' → θ. θ nucleates at θ'/matrix interface (x 70,000).

: governed by the need to reduce the large interfacial energy contribution to ΔG* for this phase

Fig. 5.31 Electron micrographs showing nucleation sites in Al-Cu alloys.

* Effect of Aging Temperature on the Sequence of Precipitates

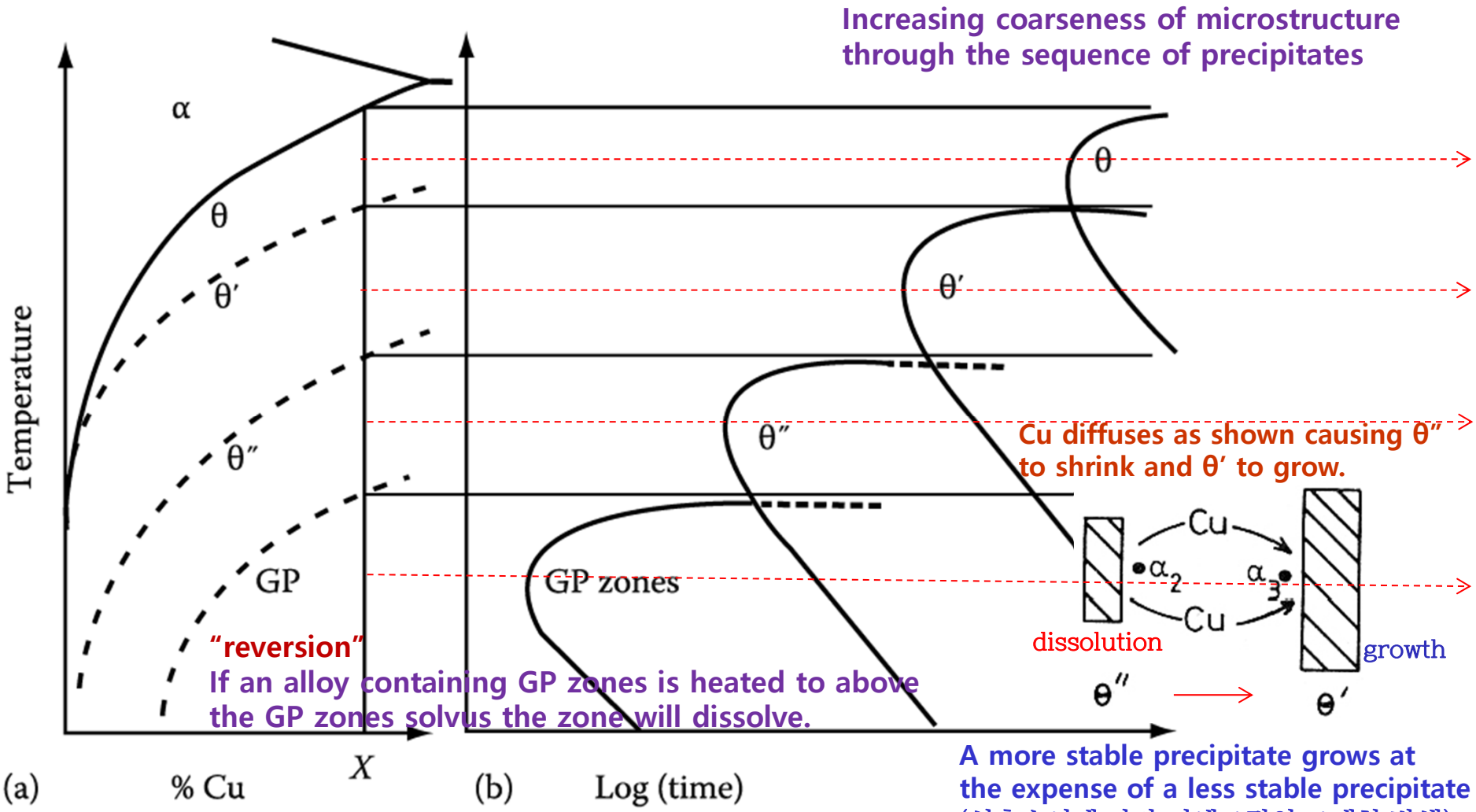

Fig. 5.32 (a) Metastable solvus lines in Al-Cu (schematic).
(b) Time for start of precipitation at different temperatures for alloy X in (a).

Q3: Age Hardening

5.5.4. Age Hardening

Transition phase precipitation → great improvement in the mechanical properties

Coherent precipitates→highly strained matrix→the main resistance to the Ⓓ movement: solid solution hardening

Hardness vs. Time by Ageing

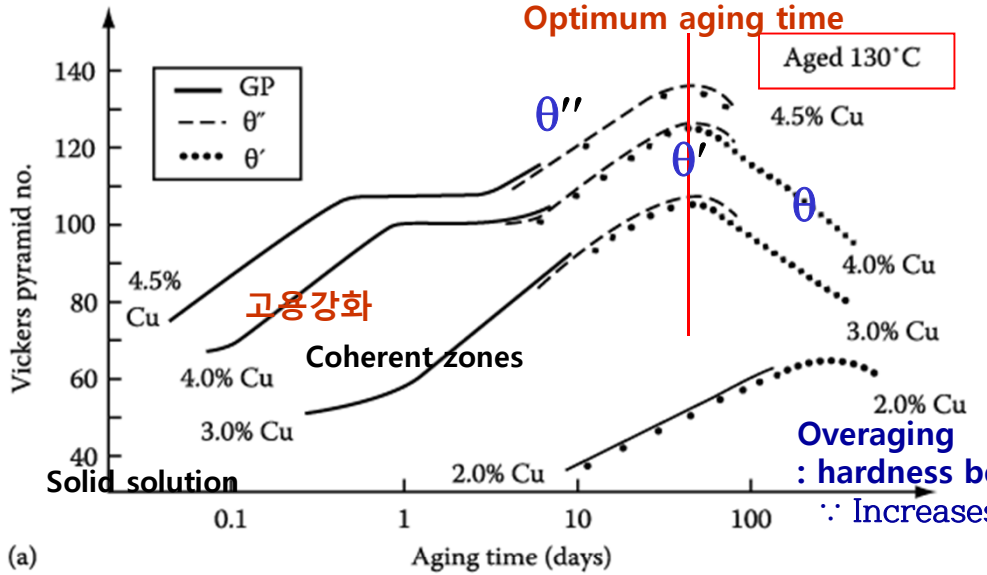

Maximum hardness~ largest fraction of θ″ (coherent precipitates)

Ageing at 130°C produces higher maximum hardness than ageing at 190°C.

At 130°C, however, it takes too a long time (several tens of days).

∵ Increases the distance btw precipitates making Ⓓ bowing easier

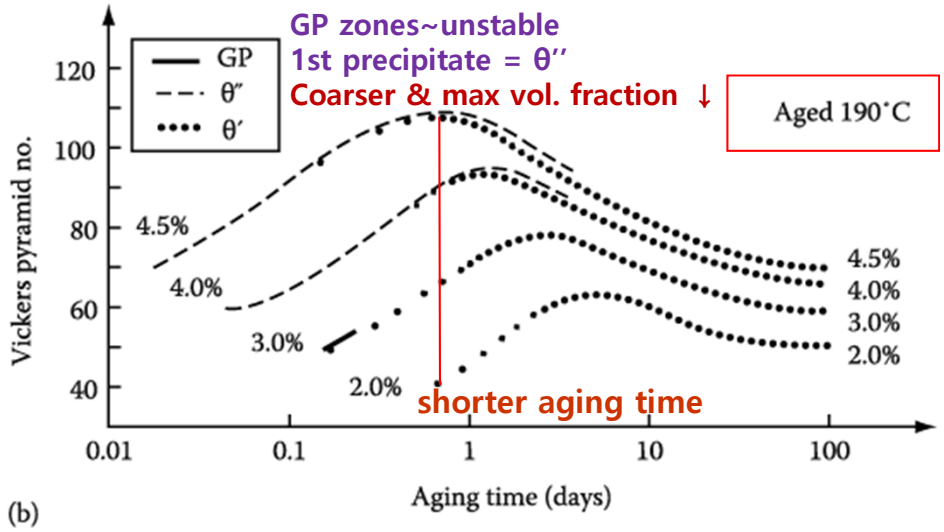

How can you get the high hardness for the relatively short ageing time (up to 24h)?

Double ageing treatment

first below the GP zone solvus → fine dispersion of GP zones then ageing at higher T.

: Engineering alloys are not heat treated for max. strength alone. → **to optimize other properties**

best heat treatment in practice

Fig. 5. 37 Hardness vs. time for various Al-Cu alloys at (a) 130 ℃ (b) 190 ℃

Q4: How can you design an alloy with high strength at high T?

Microstructure of a two phase alloy is always unstable if the total interfacial free E is not a minimum. →

5.5.6. Particle Coarsening (smaller total interfacial area→loss of strength or disappearance of GB pining effect→ particular concern in the design of materials for high temp. applications)

Two Adjacent Spherical Precipitates with Different Diameters

(Gibbs-Thomson effect: radius of curvature↓ → X_B ↑)

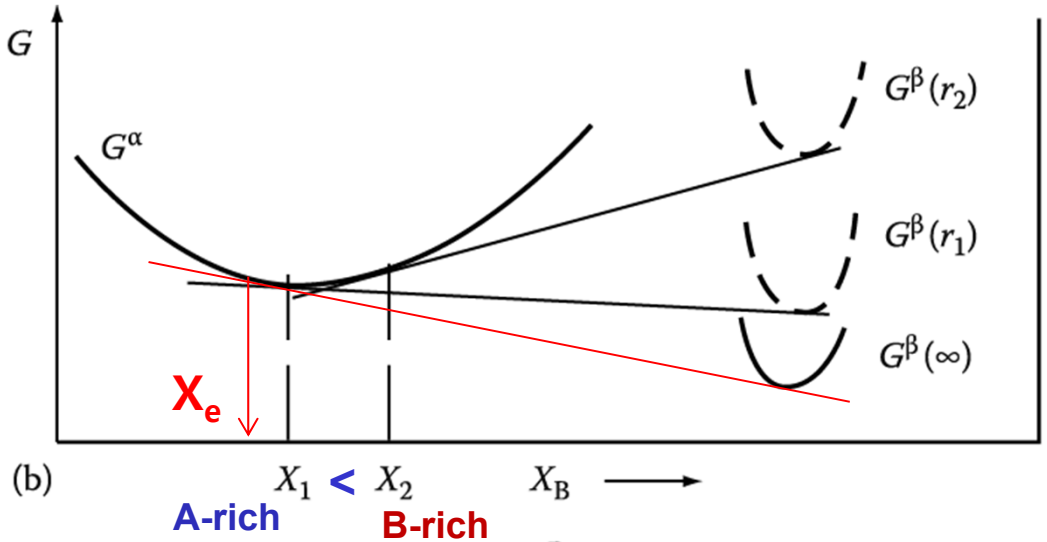

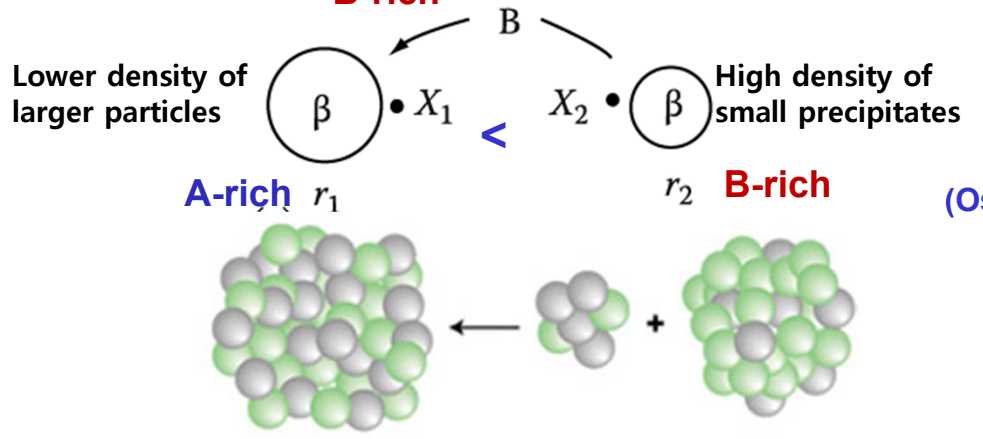

Assumption: volume diffusion is the rate controlling factor

$$\left(\bar{r}\right)^3 - r_0^{\,3} = kt$$

Average radius

where $k \propto D\gamma X_e$

(X_e: Equil. solubility of very large particles)

Coarsening rate $\dfrac{d\bar{r}}{dt} \propto \dfrac{k}{\bar{r}^2}$

(D and X_e ~ exp (-Q/RT) / $\bar{r}$ — Rapidly increase with Increasing temp.) ⇨ CR ↑

(Ostwald Ripening)

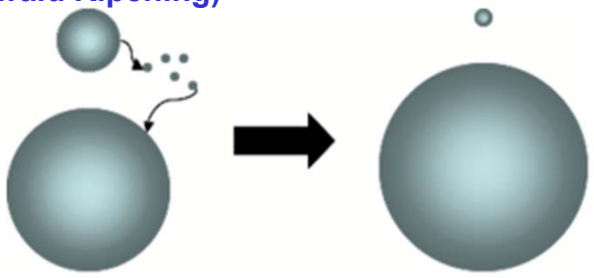

: Concentration gradient in matrix→diffusion→small particle_shrink/ large particle_grow

5.5.6. Particle Coarsening

The Rate of Coarsening with Increasing Time and Temp.

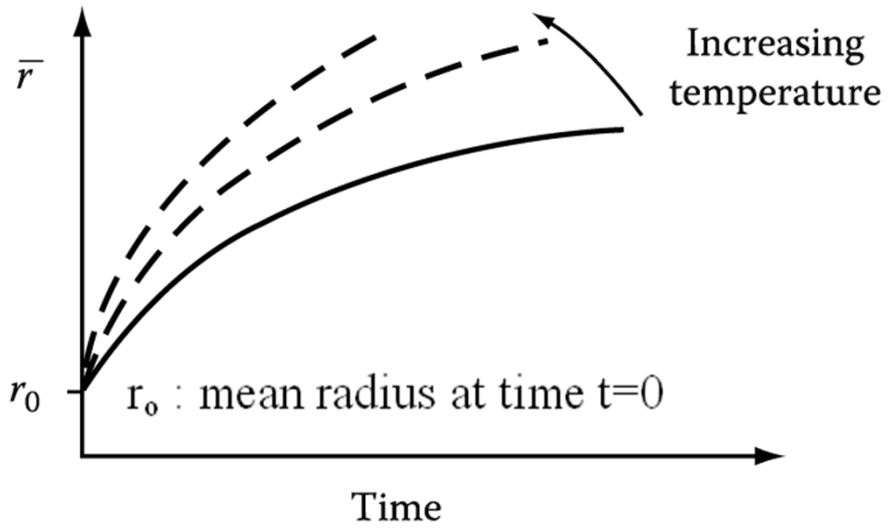

$\bar{r}$ ~ Particular concern in the design of materials for high temperature applications

Undesirable degradation of properties:
less strength/ disappearance of GB pinning effects

How can you design an alloy with high strength at high T?

→ **fine precipitate dispersion**

hint) $\frac{d\bar{r}}{dt} \propto \frac{k}{\bar{r}^2}$ $\quad k \propto D\gamma X_e$

1) low γ

heat-resistant Nimonic alloys

based on Ni-rich Ni-Cr → ordered fcc

$Ni_3(Ti,Al)$ in Ni-rich matrix → high strength

Ni/γ' interface~ "fully coherent" (10 ~ 30 mJ m^{-2})

Maintain a fine structure at high temperature

→ improve creep-rupture life

2) low X_e (Oxide~ very insoluble in metals)

: fine oxide dispersion in a metal matrix

Ex) dispersed fine ThO_2 (thoria) in W and Ni

→ strengthened for high temperature

3) low *D*

Cementite dispersions in tempered steel

→ high *D* of carbon → very quickly coarsening

a. substitutional alloying element

→ segregates to carbide → slow coarsening

b. strong carbide-forming elements

→ more stable carbides → lower X_e

Q5: Quenched-in vacancies vs Precipitate-free zone

5.5.3. Quenched-in Vacancies

If $X_v < X_v^c$ critical vacancy supersaturation,
Precipitate nucleation X → formation of PFZ

In the vicinity of grain boundaries on subsequent aging,

a) Excess Ⓥ→ Ⓓ nucleation and moving ↑:
Heterogeneous nucleation sites ↑
b) Excess Ⓥ → atomic mobility ↑ at ageing temp:
speeds up the process of nucleation and growth
ex) rapid formation of GP zones at the relatively low aging temperature. (possible to RT aging in Al-Cu alloy)

a) Precipitate-Free Zone(PFZ) due to Vacancy Diffusion during quenching

Solute concentration within the zone ~ largely unchanged, but no precipitate at GB
∵ a critical vacancy supersaturation must be exceeded for nucleation to occur.

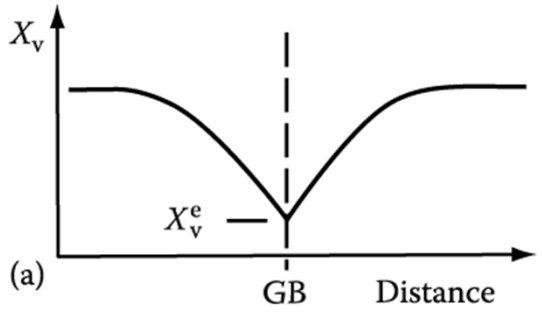

Similar PFZs can also form at inclusions and dislocations.

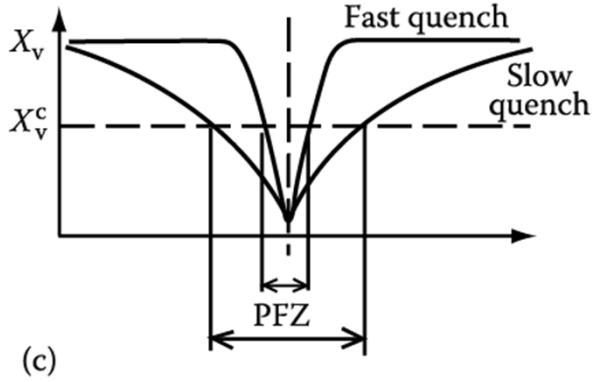

Fig. 5.35 A PFZ due to vacancy diffusion to a grain boundary during quenching.
(a) Vacancy concentration profile. (b) A PFZ in an Al-Ge alloy (x 20,000)
(c) Dependence of PFZ width on critical vacancy concentration X_v^c and rate of quenching.

* Equilibrium Vacancy Concentration

at equilibrium $\left(\frac{dG}{dX_V}\right)_{X_V = X_V^e} = 0$

$$\Delta H_V - T\Delta S_V + RT \ln X_V^e = 0$$

A constant ~3, independent of T

Rapidly increases with increasing T

$$X_V^e = \exp\frac{\Delta S_V}{R} \cdot \exp\frac{-\Delta H_V}{RT}$$

putting $\Delta G_V = \Delta H_V - T\Delta S_V$

$$X_V^e = \exp\frac{-\Delta G_V}{RT}$$

increases exponentially with increasing T

- **In practice, ΔH_V is of the order of 1 eV per atom and X_V^e reaches a value of about 10^{-4}~10^{-3} at the melting point of the solid**

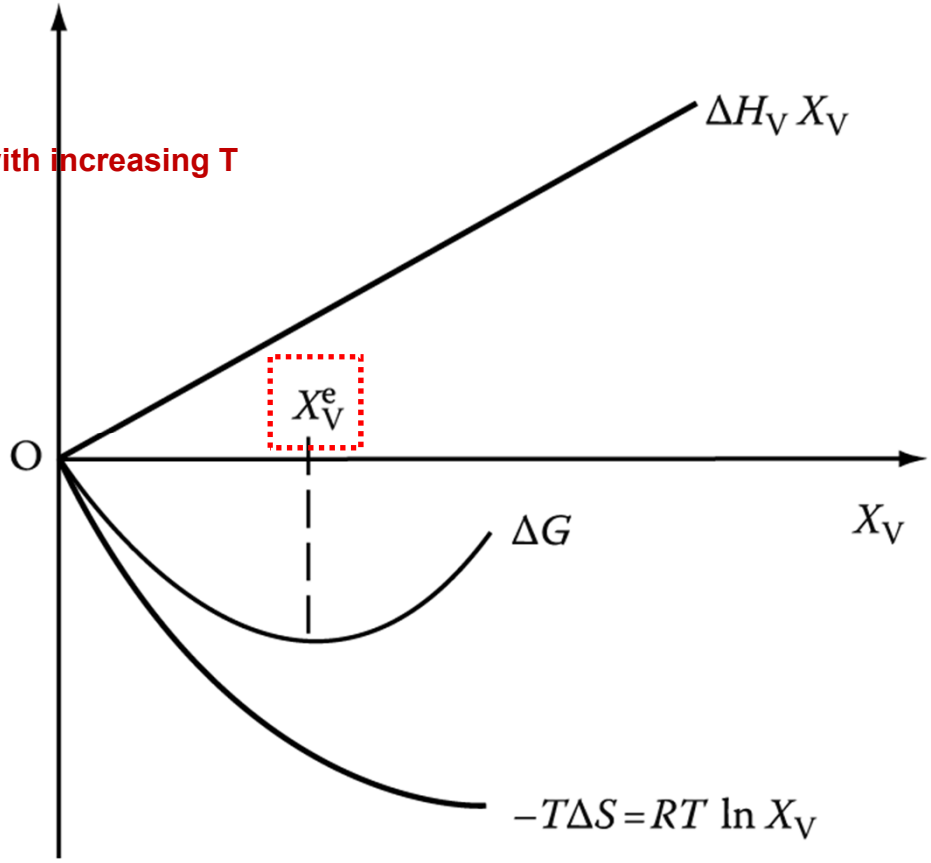

Fig. 1.37 Equilibrium vacancy concentration.

: adjust so as to reduce G to a minimum

b) Another cause of PFZs can be the nucleation and growth of GB precipitates during cooling from the solution treatment temperature.

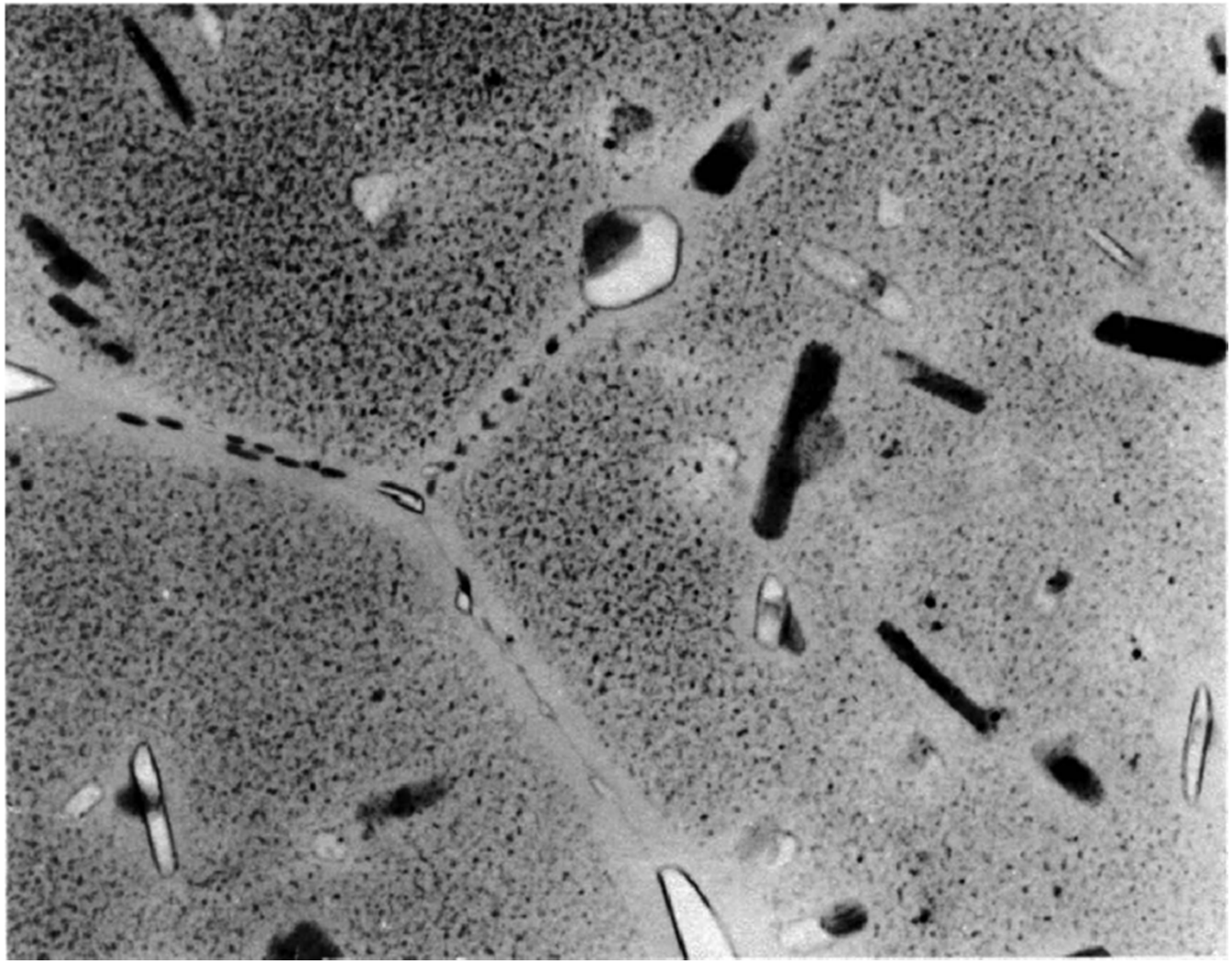

Fig. 5.36 PFZs around grain boundaries in a high-strength commercial Al-Zn-Mg-Cu alloy. Precipitates on grain boundaries have extracted solute from surrounding matrix. (x 59,200)